ABSTRACT

Title of Thesis: STRANDED AND SANDED IN: DRONE MOUNTED AERIAL MAGNETOMETER IDENTIFICATION OF BURIED AND SUBMERGED SHIPWRECKS ON THE NEW JERSEY COAST

Cullan Matthew Davis, Master of Professional Studies, Cultural and Heritage Resource Management, 2022

Thesis Directed By: Dr. Matthew M. Palus, Anthropology Department

An estimated 3,000 to 7,000 shipwrecks have occurred off the coast of New Jersey, with hundreds occurring within the littoral zone. These sites have subsequently been buried by natural sand movement and beach replenishment projects or exist in a partially buried state within the surf zone. While terrestrial and vessel-mounted magnetometer surveys are not feasible in this shallow environment, the development of ultra-sensitive drone and unmanned aerial vehicle (UAV) based remote sensing platforms has provided the potential ability to rapidly identify these cultural materials for compliance and planning of weather and climate change resiliency projects. This thesis proves the capabilities of a MAGPi ML-4 atomic magnetometer, initially designed to detect small, buried munitions and unexploded ordinance of approximately eight pounds of ferrous material, to accurately and rapidly identify multiple of types of shipwrecks in the high energy coastal environment where traditional survey methods are

precluded when coupled with a Matrice 600 Pro 6-rotor drone. This thesis also proved the ability for this setup to effectively bridge the gap between terrestrial and underwater archaeological surveys as presented in the littoral zone, while producing data of sufficient quality to promote the development of the theoretical understanding of the relationship between shipwrecks and the larger maritime cultural landscape.

Three shipwrecks were used for data collection, representing vessels comprised of iron, wood, and steel. Additional measurements of individual ferromagnetic objects commonly found in association with shipwreck archaeological sites were taken and analyzed using predictive modeling based on magnetic detectability algorithms created from prior remote sensing surveys to determine what material can be detected using the magnetometer and UAV platform. The results of this thesis confirm the predicted capabilities of the equipment used and provides detection ranges to establish a framework to future research, including a determination on the minimum amount of wooden hull material with iron fasteners required to exist in an archaeological context to be detectable.

STRANDED AND SANDED IN: DRONE MOUNTED AERIAL MAGNETOMETER IDENTIFICATION OF BURIED AND SUBMERGED SHIPWRECKS ON THE NEW JERSEY COAST

by

Cullan Matthew Davis

Thesis submitted to the Faculty of the Graduate School of the University of Maryland, College Park, in partial fulfillment of the requirements for the degree of Master of Professional Studies, 2022

Advisory Committee:
Dr. Matthew M. Palus, Chair
Associate Professor George Hambrecht
Associate Professor Kathryn Lafrenz Samuels

Acknowledgements

First, I would like to acknowledge the tremendous support and assistance from Dr. Martin Helmke of West Chester University, whose technological skill, passion for and access to UAV technology, and encouragement made this project possible. At the same time, I would also like to acknowledge the assistance from Dr. Greg Schultz, who provided his time, his magnetometer, and his analytical skills and software for this project. Third, I would like to acknowledge the technical support and magnetic calculation spreadsheets provided by Matt Hanks of the National Park Service Submerged Resources Center.

I would like to thank Dr. Matthew Palus of the University of Maryland for his encouragement and guidance throughout the development of this thesis and the entirety of the University of Maryland program, as well as my thesis committee, Dr. George Hambrecht and Dr. Kathryn Lafrenz Samuels.

My supervisors have afforded me tremendous flexibility to achieve my academic pursuit. I would like to thank my former supervisors, Assistant Chiefs Ryan Geraghty and Michael Cameron of the United States Coast Guard Fire Department at Training Center Cape May. I would also like to thank my current supervisors in the National Park Service at Valley Forge National Historical Park, namely Dr. John Turck, Park Archeologist, and Amy Ruhe, Chief of Planning and Resource Management.

Finally, I would like to thank my wife Rosalyn for her support of my academic and career pursuits.

Table of Contents

Acknowledgements ii
Table of Contents iii
List of Tables v
List of Figures vi
Chapter 1: Introduction 1
Chapter 2: Theoretical Background 2
2.1 The Development of Theory in Maritime Archaeology 5
2.2 Formation Theory 8
2.3 Theoretical Views of the Maritime Cultural Landscape 10
Chapter 3: Environmental and Historical Background 12
3.1 The Challenging Environment of the Littoral Zone 12
3.2 127 Miles of Shipwrecks 14
3.3 The Malta 17
3.4 The Rjukan 18
3.5 The Sindia 19
Chapter 4: Methods and Data Collection 21
4.1 Technological Development 21
4.2 Site Selection Criteria 23
4.2.1 Criteria 1: Location 24
4.2.2 Criteria 2: Previous Site Identification 24
4.2.3 Criteria 3: Legality of UAV Operations 25
4.3 Safety Considerations 25
4.4 Pre-Flight Operations 25
4.5 Site Specific Flight Operations 27
4.5.1 The *Malta* 27
4.5.2 The *Rjukan* 28
4.5.3 The *Sindia* 29
4.6 Additional Data Sources 32
Chapter 5: Results 34
5.1 Aerial Magnetometer Surveys 34
5.1.1 The *Malta* 34
5.1.2 The *Rjukan* 36
5.1.3 The *Sindia* 38
Chapter 6: Analysis 42
6.1 The Malta 42
6.2 The Rjukan 47
6.3 The Sindia 49
6.4 Additional Ship Material 52
6.4.1 Mass Specific Magnetic Moment 54
6.4.2 Corrected Maximum Detection Range 58
6.4.3 Vertical Distance and Transect Interval 59
6.4.4 Superposition of Magnetic Fields 62
Chapter 7: Conclusion 66

7.1 Operational Capabilities.. 66
7.2 Detectability.. 68
7.3 Limitations.. 69
7.4 Future Applications.. 72
Bibliography.. 74

List of Tables

Table 1**.** Ship fitting measurements for magnetic detectability determination 55
Table 2. Ship armament measurements for magnetic detectability determination..... 57
Table 3. Ship ammunition measurements for magnetic detectability determination from Collins (n.d.)... 58
Table 4 Ship anchor weights from Historic Naval Ships Association (2022) .... .58
Table 5**.** Determination of distance between target and magnetometer sensor at given flight and transect parameters. 61
Table 6. Relative estimation of densities of ferromagnetic fasteners in surviving hull material 63

List of Figures

Figure 1. NOAA AWOIS (Automated Wreck and Obstruction Information System) map of charted shipwrecks along the New Jersey coast 16
Figure 2. Image depicting the *Malta* as the *Queen of the South* and with the original steam engine 17
Figure 3. Image depicting the *Sindia* aground 19
Figure 4. Matrice 600 Pro 6-rotor drone with MAGPi ML-4 on carbon fiber rod 22
Figure 5. Matrice 600 Pro 6-rotor drone with MAGPi ML-4 on carbon fiber rod in flight 23
Figure 6. *Malta* flight area, camera facing northeast 28
Figure 7. *Rjukan* flight area, camera facing northeast 29
Figure 8. *Sindia* survey area, camera facing northeast 30
Figure 9. Handheld magnetometer data collection for the *Sindia,* carried by an undergraduate student from West Chester University 31
Figure 10. Handheld magnetometer data collection transects for the *Sindia,* carried by an undergraduate student from West Chester University 31
Figure 11. *Malta* 3D magnetometer data profile 35
Figure 12. *Malta* 2D 30 nT scale grid 35
Figure 13. *Rjukan* 3D magnetometer data profile 36
Figure 14. *Rjukan* 2D 5 nT scale grid 37
Figure 15. *Rjukan* 2D 10 nT scale grid 37
Figure 16. *Rjukan* 2D 30 nT scale grid 38
Figure 17. *Sindia* 3D magnetometer data profile 39
Figure 18. *Sindia* 2D 10 nT scale grid 39
Figure 19. *Sindia* 2D 30 nT scale grid 40
Figure 20. *Sindia* 2D 50 nT scale grid 40
Figure 21. The sternpost of the *Malta* visible in the lower left-central of the photo .. 43
Figure 22. 30 nT map showing with dipole anomaly showing the location and orientation of the iron-hulled, full-rigged ship *Malta* 44
Figure 23. Image depicting the *Malta* breaking apart. The sternpost, still visible to this day, is the dark object protruding from the water in the lower left portion of the photo 45
Figure 24. Photo of the stern and ribs of the *Malta* during an extremely low tide with camera facing west 46
Figure 25.10 nT map showing with dipole anomaly showing the location of the wooden-hulled *Rjukan* 47
Figure 26. 10 nT map showing with dive sketch overlay showing the location of the *Rjukan* anchor in relation to the magnetic anomalies 49
Figure 27. 1933 aerial photograph showing hull components of the *Sindia* 50

Figure 28. 30 nT magnetometer data overlay of georeferenced historic aerial photograph of the *Sindia* shipwreck 51

Chapter 1: Introduction

Changes in sea level have, and are projected to continue to, significantly and detrimentally impact buried and submerged cultural resources around the world. As public engineering projects continue to be developed and implemented in the United States and elsewhere, there is an urgent need to develop the capability to complete archaeological surveys to identify potentially impacted cultural materials in environments that preclude traditional survey methods, such as deeply buried sites in sand and those that exist in both the buried and submerged context of the high-energy surf zone, presenting not only a hazard to divers and boats, but no visible surface relief for side-scan sonar. Can an unmanned aerial vehicle (UAV) provide an efficient, safe, and practical platform to deliver a magnetometer payload to conduct remote sensing in the near-shore, dune, and high-energy surf zone of the maritime environment for the identification of multiple types of shipwrecks? Furthermore, how can the use of UAVs bridge the gap between terrestrial and underwater archaeology to identify a broad range of historic cultural resources that face degradation and loss due to changing coastal environments? Is the data generated from this type of survey of sufficient quality to contribute to the development of a theoretical understanding of the relationship between shipwrecks, the sea, and socioeconomic relationships of the past?

Recently, several infrastructure projects have unintentionally impacted unknown shipwreck locations, causing significant damage to irreplaceable archaeological resources. During the summer of 2014, the United States Army Corps of Engineers initiated a project to repair damage to the north jetty of Barnegat Inlet near Long Beach Island, New Jersey. During the reconstruction, crews utilizing heavy machinery to remove the existing, damaged jetty disturbed wooden and metal pieces of an early 20th century schooner buried beneath the 1930's-era jetty (James, Jr. & Gifford, 2015:i). During October of 2014, workers installing steel sheeting as part of a coastal flood prevention infrastructure project in Brick Township, New Jersey damaged a wooden and iron shipwreck buried approximately twenty-five feet beneath the sand (CBS New York 2014).

Storm damage and erosion present additional impacts on unknown and unrecorded archaeological sites in the maritime cultural landscape. Superstorm Sandy removed over seventy linear feet of sand and dunes from Fire Island National Seashore, uncovering the remains of the *Bessie White*, lost in the early 1900's (O'Connor 2012). In 2019, multiple shipwrecks were uncovered due to high tides along the shores of Lake Michigan (Jaworski 2019), including a 19th century scow uncovered by storm surge off Muskegon, Michigan (White 2019). In 2020, a storm in northeastern Florida removed an estimated ten feet of sand from the beach, uncovering the remains of a 19th century shipwreck and leading to a data recovery race against the clock before the next engineering project covered the shipwreck with sand (Saraceni 2020). The ability to identify these resources prior to being impacted by adverse environmental conditions will provide archaeologists and land managers the capability to target resources during post storm surveys and monitor maritime cultural resources more efficiently.

While there is a clear need to identify and document the locations of maritime cultural resources as the risk for potential adverse impacts continues to grow, this thesis does not seek to evaluate the use of UAV-mounted magnetometers and remote sensing equipment capabilities in environments well-suited to towed magnetometer arrays and side-scan sonar. Instead, it seeks to determine the capabilities of high precision magnetometers delivered via UAV in coastal environments unfavorable to other survey methods to identify these vulnerable resources. It is expected that this thesis will confirm the ability to accurately detect significant components of multiple types of shipwrecks and other historic cultural resources that exist within the maritime cultural landscape of New Jersey. Prior testing completed by Dr. Martin Helmke and Dr. Greg Schultz have proven the capabilities of the specific magnetometer and UAV equipment used for this thesis to locate unexploded ordinance weighing between 0.4 kg and 32.1 kg at a distance of 1.7 m and 4.8 m respectively (Schultz et al. 2021). Given these previously obtained results, it is reasonable to expect that the equipment used in this thesis will be able to detect the significant iron and steel remains of shipwrecks within the survey areas from a distance greater than ten meters. It is also expected that significant iron components of wooden-hulled shipwrecks, such as anchors and structural iron pins, will also be detected at a distance greater than ten meters. Even if small iron objects are present, the cumulative mass and relative densities should provide an acceptable target for magnetometer detection.

Chapter 2 of this thesis seeks to provide an overview of the development and application of theory to maritime archaeology, including the works of Meide, Gould, and Muckelroy. Formation theory is then discussed, with special focus on how natural and cultural transforms have affected the archaeological sites of this project. Finally, the role of shipwrecks within the broader context of the maritime cultural landscape is expanded upon, allowing for understanding on how shipwrecks are components of broader cultural traditions.

Chapter 3 delves into the rich maritime history of New Jersey, with an explanation of how thousands of vessels ended up in this “Graveyard of the Atlantic”. Details are presented related to the construction and events leading to the loss of three specific ships used to evaluate magnetometer application in this thesis, the shipwrecks of the *Malta*, *Rjukan*, and *Sindia*.

Chapter 4 details the specifications of the MAGPi ML-4 magnetometer used for data collection and the Matrice 600 Pro 6-rotor drone used to deliver the magnetometer over the survey area. Chapter four also details the site selection criteria developed for the thesis, safety considerations, pre-flight details, and specifications on the data collection at each location. Chapter 4 concludes with an evaluation of additional data to fill in gaps exposed during the project.

Chapter 5 describes the results of the magnetometer surveys of each location, including 3D data profiles and flight grids generated by Dr. Greg Schultz from thesis flight data. Chapter 6 further develops the results in chapter five into two distinct deliverable outcomes. The first outcome is the application of visual overlays to the shipwreck locations, coupled with historic images and diver sketches to correlate the magnetometer data and validate the effectiveness of the magnetometer and UAV ensemble to correctly detect cultural material in the project environment. The second outcome is the use of mathematical equations to develop predictive capabilities of the magnetometer and UAV ensemble to determine the minimum detection altitude of common ephemeral ferromagnetic components of shipwrecks to answer questions of detectability and applicability that this project was unable to directly provide.

Finally, Chapter 7 details a summary of the capabilities, detectability, limitations, and future applications for the employment of this magnetometer and UAV setup in future projects. It is the hope of the author that future researchers will expand upon the capabilities and datasets presented in this thesis for the protection and understanding of our critically important, imperiled, and endangered maritime cultural resources.

Chapter 2: Theoretical Background

2.1 The Development of Theory in Maritime Archaeology

In 1990, Gibbins (1990:383) stated that there was a "relative scarcity in this field of scholars who are strongly conversant with prevailing archaeological method and theory." Meide attempted to explain the lack of theoretically engaged maritime archaeologists as a combination of a dissimilar theoretical basis from mainstream archaeologists, as well as the fact that the professional field of underwater and maritime archaeology was still young. While the basis of individuals in maritime archaeology came from a strong and well-suited interdisciplinary background, few were trained as classicists or medievalists, and fewer still were engaged with the discourse of archaeological theory (Meide 2013:7). Instead, the majority of maritime archaeologists focused on the development of new technologies, methods, and understanding shipwreck construction and typologies (Adams 2003:7). In their defense, Bass (1982:97-98) made the argument that data collection and classification to build a body of knowledge for a new field is a prerequisite for any theory development. Jonathan Adams (2003:6) summarized that the only way that the new "sub-discipline" of maritime archaeology could contribute to archaeology would be to develop an appropriate methodology, in order to break free of an association with antiquarianism and treasure salvage. He further stated that this process needed to include not only the physical excavations, but also the recording, conservation, and post-excavation analysis of material, as there was a very real sense of the need to catch up to terrestrial archaeology and demonstrate credibility through the development of high-quality data to support the field as valid research (Adams 2003:6).

Meide described the development of a processual approach to maritime archaeology that came from Keith Muckelroy in the 1970's and 1980's and his influences from prehistoric and analytical archaeology from Cambridge. Muckelroy focused on the understanding of the formation processes of underwater archaeological sites, developed terms to describe the environmental components that disarticulated some shipwreck sites, and used statistical models to discern patterns in the wrecking process of ships (Meide 2013:8-9). Muckelroy focused on working the specific wrecking process that created a shipwreck backwards from the initial moment of the shipwreck event to model the relationship between object location and the original location within the ship, in order to understand the wrecking, salvage, natural disintegration, movement and excavation influences on the material remains of a shipwreck (Flatman & Staniforth, 2006:170-171). He further worked within the processual approach of analytic and scientific methodology by developing a three-part framework for the interpretation of the original social context of a ship, consisting of the ship as a machine to harness a source of power as a means of transport, the ship as an element in an economic or military system, and the ship as a closed community that consisted of customs, hierarchy, and conventions (Muckelroy 1978:216). Meide wrote that the processual approaches of Muckelroy were further developed by George Fischer of Florida State University, who used a systematic grid system and stratified sampling strategy to excavate and identify artifact patterning on the wreck of the HMS Fowey in Biscayne National Park in 1983. Meide stated that as a professor, Fischer continued to encourage the use of processual quantitative patterning statistical analyses for shipwreck sites amongst his students. Processual based underwater archaeology was further supported by Richard Gould of Brown University, who organized a seminar called "Shipwreck Anthropology" and brought together other processualists, such as Daniel Lenihan and Larry Murphy of the National Park

Service and Patty Jo Watson to discuss the lack of hypothetico-deductive research designs in underwater archaeology, resulting in the publication of the book *Shipwreck Anthropology* (Meide 2013:9). Gould proposed conducting shipwreck archaeology from a cultural anthropology standpoint based on cultural relativism, cultural presentism, and cross-cultural comparison, instead of classical studies (Flatman & Staniforth, 2006:170).

Post-processual views have increasingly factored into the development of underwater archaeology since the 1980's. Post-processualism presented a sense of increased theoretical receptiveness instead of a defined methodology, combining models, approaches, and ideas along with input from a variety of disciplines, including inductivism and historical particularism (Gibbins & Adams, 2001:286). Adams phrased the emergence of post-processual themes as a refreshing re-assertion of the roles of individuals in archaeology and the past, with a closer link between underwater archaeology and symbolic and contextual archaeological themes. He criticized Hodder by stating that material culture was not the fossilized action of the past, but active and possessing of more than one meaning, supported by the rich assemblages found on shipwrecks (Adams 2003:14).

Another theme in the development of post-processual theory in maritime archaeology since the 1990's has come from Europe and Scandinavia, with a focus on the idea of shipwrecks and the maritime cultural landscape, defined by Christer Westerdahl and described by Meide. As stated by Meide, Muckelroy defined maritime archaeology as "the scientific study of the material remains of man and his activities on the sea", however he specifically excluded "related objects on the shore" and "coastal communities". This limited focus on ships, shipwrecks and their associated onboard communities were seen as too narrow, as they excluded the connections to cultural materials in coastal, shoreline and riverine locations that contributed to the overall study of maritime heritage (Meide 2013:12). Westerdahl (1986, 1992) thought of the maritime landscape as a more encompassing understanding of broader cultural themes. Westerdahl defined the maritime cultural landscape as "the whole network of sailing routes, with ports, havens, and harbors along the coast, and its related constructions and other remains of human activity, underwater as well as terrestrial", signifying "human utilization (economy) of maritime space by boat: settlement, fishing, hunting, shipping, and its attendant sub-cultures, such as pilotage, lighthouse and seamark maintenance" (Meide 2013:12).

2.2 Formation Theory

The focus of this thesis is on shipwrecks in the shallow water environment, subjected to environmental and anthropogenic scattering and destruction, and exhibiting site characteristics more similar to terrestrial sites, and less like the 'time capsule' characteristics of some deep-water locations. Shipwrecks are unique events, formed from individual actions and local circumstances, that results in the particular deposition of remains in a specific context, subjected to storms, waves, looters, woodworms, and reef building (O'Shea 2002:211). These effects, coupled with the use, loss, deposition, identification, and potential recovery of shipwreck material, comprises the main components of the 'formation theory', as discussed by Schiffer (O'Shea 2002:211-212). By understanding the components of formative theory on New Jersey shipwrecks in the surf zone, understanding of how and what occurs during the transitional phase where shipwrecks pass from the systemic, behavioral context to an archaeological, static context as identified in this thesis can be understood.

One subsect of formative theory, termed depositional theory, relates to how an object, in this case a ship, becomes part of the archaeological record, through understanding of whether the wrecking event occurred intentionally, due to human error, or due to natural events (O'Shea

2002:212). This concept is especially important when understanding the causations of New Jersey shipwrecks. Human error in navigation, poor judgement during inclement weather, failure of shore-based optical navigation systems, intentional grounding, and weather events have all contributed to the accumulation of cultural material. Conlin discusses how ship construction techniques, repairs, alterations, vessel use, and pre-wreck conditions of the vessel all influence the pattern of pre-depositional conditions that lead to the site formative event (Conlin 1998). By separating shipwreck events into specific categories based on the type of final disposition, the characteristics of a depositional pathway can allow the identification of the shipwreck process, allowing additional site formation processes to be inferred (O'Shea 2002:213).

The post-depositional theory subset of formative theory relates to what is or is not preserved and how a shipwreck is redeposited and modified through natural processes and anthropogenic, often culturally significant, activities (O'Shea 2002:212). The New Jersey coastal environment is dynamic and changing, with seasonal fluctuations in water temperatures, shifting sandbars and migrating beaches. Most historic shipwrecks off New Jersey can be characterized by low-lying hull components, machinery, and cargo, with rigging components rarely seen. Wrecks that are visible one year may be completely covered by marine sediments in the following season, with implications for the preservation of organic materials due to burial and exposure reflected in the site characteristics. Storm surges and wave action, often factors in the site formation process and initial deposition, can work vessels across sandbars, change ship orientation, and scatter wreck materials well beyond the initial wrecking site. Rigging, spars, deck material and structural components of shipwrecks are often swept clean from the vessel, resulting in a lack of this material in the archaeological context. Wrecking, a coastal human activity concerned with the salvage of a ships' structural materials, cargo, rigging, and occasionally the destructive salvage of the entirety of the hull, all influence the physical characteristics of shipwreck sites, as does modern looting. These human factors are a key component to many maritime communities, who obtained building components for houses and other commodities through the official wreck salvaging process.

The final subcomponent of formation theory, recovery theory, has significant implications for this project. Recovery theory seeks to understand how a site is discovered, including which components are recorded and recovered, and the subsequent implications on the bias of site interpretation (O'Shea 2002:214). This implies that some sites are not discovered or recorded, potentially due to search techniques, leading to incorrect conclusions from data analysis. This project seeks to understand the capabilities of a specific type of magnetometer to identify shipwreck sites that are precluded from traditional survey methods. A lack of ferro-magnetic material on a wreck site, due to depositional and post-depositional theoretical influences, may result in a failure to identify shipwreck locations, leading to an unintentional analytical error of resultant data.

2.3 Theoretical Views of the Maritime Cultural Landscape

The maritime cultural landscape can be described as the combination of the physical aspects of the seascape and the landscape that allows for the analysis of the spatial context of maritime cultures while still understanding the culture-nature relationship that can be seen in terrestrial landscapes, expressed through the study of physical remains of lighthouses, shipwrecks, wharves, and other cultural features (Ford 2011:4-5). Understanding the concept of a broader cultural landscape that includes shipwrecks allows for the interpretation of the shipwreck as more than a singular isolated feature and set of artifacts, but instead as a component of a broader cultural framework (Keith & Evans 2011).

It is imperative to understand the fundamental principles of the maritime cultural landscape model to understand the sites and site formation processes of this project area. The density of shipwrecks in New Jersey is a product of the border maritime cultural landscape of the New Jersey, New York, and the mid-Atlantic Seaboard, which is expanded upon in the historical context chapter of this thesis. The coastline of New Jersey exists along the major shipping route of goods from cities such as Philadelphia, Wilmington, and New York, and incorporates international shipping and transport of goods and people, including immigrants destined for New York. These transportation routes relied on recognition of landforms, inlets, and lighthouses as they navigated the shifting sandbars and shoals of the region. Local shipbuilding on the Delaware Bay was supplemented by vast stands of cedar available locally, a prized commodity for ship building, leading to numerous shipyards in the region. Hurricanes, nor'easters, and fog all work to create seasonal hazards to maritime transport. The type, distribution, and wrecking circumstances of the vessels identified for this project are components of the broader New Jersey maritime cultural landscape and exist as products of this cultural-natural relationship. By understanding the environment and historical background of maritime New Jersey, we can begin to understand how the diverse remains of ships within this area can contribute to the broader understanding of the relationship between mankind and the sea.

Chapter 3: Environmental and Historical Background

3.1 The Challenging Environment of the Littoral Zone

The area of focus of this thesis exists in an archaeological "in-between" zone, straddling terrestrial sites and true underwater resources. Containing a dynamic dune environment, tidal depth fluctuations, high-energy breaking surf, estuaries, and bays, it is best defined as the littoral zone, an area which includes tidal and longshore currents, water depths up to approximately thirty feet, rocky coasts, coral reefs, and sandy beaches that can extend hundreds or thousands of feet in width (Encyclopedia Britannica, 2019). Physically, this zone provides the tangible link between the maritime world of seagoing vessels and the land-based infrastructure and settlements they support and the influences of the sea over the land. Culturally speaking, this zone contains not only shipwrecks, but the remains of wharves, lighthouses, fortifications, and materials of the broader maritime cultural landscape. By understanding how the remains of shipwrecks and other cultural resources in the littoral zone relate to the cultural landscape, we can understand how they fit into the larger political, economic, and social aspects of the historical timeframe of their loss (Horlings 2014:45-54). The littoral zone and associated seascape connect the activities and behaviors of social groups, including trade, international relations, and daily life with the cultural components of human interaction within this zone, creating a repository of physical remains (Horlings 2014:98).

Cultural resource surveys present significant challenges in this area. In South Africa, a marine magnetometer search for the slave ship *Meermin* was significantly limited due to the inability to get close to shore, excluding a large area from the survey (Boshoff 2018:45). A 2002 survey of cultural resources in U.S. Virgin Islands National Park contained multiple areas where shallow depths of less than four feet prevented magnetometer survey, along with areas where shallow coral heads could have damaged towed arrays (Richards 2016: 40-46, 55). In the Wadden Sea, investigations on an exposed shipwreck normally covered with sand were limited to a one-hour window at extreme low tide, and only once every few months with offshore winds blowing favorably (Zwick 2021:203).

Sites in these zones are at risk or storms and rising sea levels. The shipwreck in the Wadden Sea became visible following sand dunes moving at a rate of over fifty meters a year, resulting in the shipwreck being completely destroyed by the sea within two months, with only two days of fieldwork completed (Zwick 2021:203-204). Areas of the estuary of the Severn River, which contains dozens of shipwrecks, have been identified as locations that could experience “major change” over the next century from a shifting coastline (Ashwell 2020:6). A shipwreck uncovered in Stone Harbor, New Jersey, and visited by the author of this thesis in 2019 was completely destroyed by a storm in 2022. Owning to this dynamic environment, a survey from Maryland to Delaware in 2013 recommended a periodic survey owning to the action of storms, tides, and currents on sediments, potentially exposing currently unknown and undetectable shipwreck sites (Jordan 2014:74).

While the littoral zone and areas of study for this thesis may appear to only contain fractured and disarticulated cultural remains, a survey in Channel Islands National Park found that shipwrecks located in the intertidal zone and above the high tide mark contain important and reliably interpretated archaeological data (Russell 2002:369). While some heavier items and ferromagnetic components, such as iron fasteners in timbers, boiler components, and pieces of the windlass can become separated from hull materials, other components can become rapidly buried and well preserved, as was seen with the remains of the Comet (Russell 2002:370-374).

This reinforces the archaeological importance of shipwrecks within the littoral zone, including those found along the New Jersey coast.

3.2 127 Miles of Shipwrecks

The coast of New Jersey has presented hazards to shipping and navigation for over three hundred years. Situated between two of the busiest shipping ports in the nation, New York City and Philadelphia, the New Jersey coast has incurred an estimated three to seven thousand shipwrecks during this time, with the earliest known example occurring after a storm in 1640 (Downey 1983:3). Within this region, few ports or harbors of safety exist; Manasquan, Barnegat, and Absecon Inlets all have hazardously shifting shoals, sandbars and channels guarding their approaches (James, Jr. & Gifford 2015:18). As a response to nearly 338 recorded shipwrecks between 1839 and 1848 alone, a series of Federally funded and constructed lifesaving service stations were installed along the desolate and often uninhabited shoreline of New Jersey (Noble 1994:21). Starting as a volunteer service manned by local fisherman and pilots, lifeboat stations were expanded along the entire New Jersey coast with a station placed for every five miles of coastline, increasing to forty-two stations, one for every three miles, by 1886 (James, Jr. & Gifford 2015:18-19). Forming the United States Life-Saving Service (USLSS), these stations were originally manned April to November and later year-round by a professional, paid staff. In 1915, the Life-Saving Service merged with the United States Revenue Cutter Service to form the current United States Coast Guard. Only nineteen of these stations remain today, with three open to the public.

To assist in combatting the deadly shoals and inlets of New Jersey, a series of light stations were built along the coast, starting with the privately funded construction of Sandy Hook Lighthouse in 1761 (James, Jr. & Gifford 2015:24). Other lighthouses were constructed at Cape

May, Hereford Inlet, Absecon, Barnegat, Tucker's Island, Sea Girt, and Navesink. The lighthouse at Barnegat was built to assist navigation, as it exists one mile south of the fortieth parallel, a critical location for ships coming from Europe that would sail west along the fortieth parallel until sighting land, then make a hard turn to the north to enter New York. It has been estimated that the shoals around Barnegat alone claimed up to forty ships per year, with losses of life possibly exceeding five hundred persons (James, Jr. & Gifford 2015:25).

While the lighthouses and remaining U.S. Life-Saving Service stations remain as tangible links to the maritime history of New Jersey, the buried and submerged remains of shipwrecks, the reason for the construction and establishment of the former, exist beneath the beach and water surface of most coastal areas of New Jersey. Occasionally revealed after a storm or caught by a trawler, the rich shipwreck assemblage of New Jersey represents a multitude of vessel construction types, ship purpose, and eras of design.

According to a public database maintained by the New Jersey Maritime Museum, data exists for 4593 recorded shipwrecks from the years 1705-2020 lost off the coast of New Jersey (New Jersey Maritime Museum 2021) (Figure 1). Of these, 1363 shipwrecks have hull construction materials listed. Eighty-one are listed as being constructed of iron, 999 are listed as being constructed of wood, and 266 are listed as steel. Additionally, one is listed as "oak/iron", one is listed as "wood and metal", one is listed as "wood or steel", two are aluminum, one is concrete, nine are fiberglass, one is "full model", and one is listed as "blimp". In order to adequately reflect the varied construction techniques of hull material represented through three hundred years of shipbuilding and loss, three specific shipwrecks were identified as targets for this project.

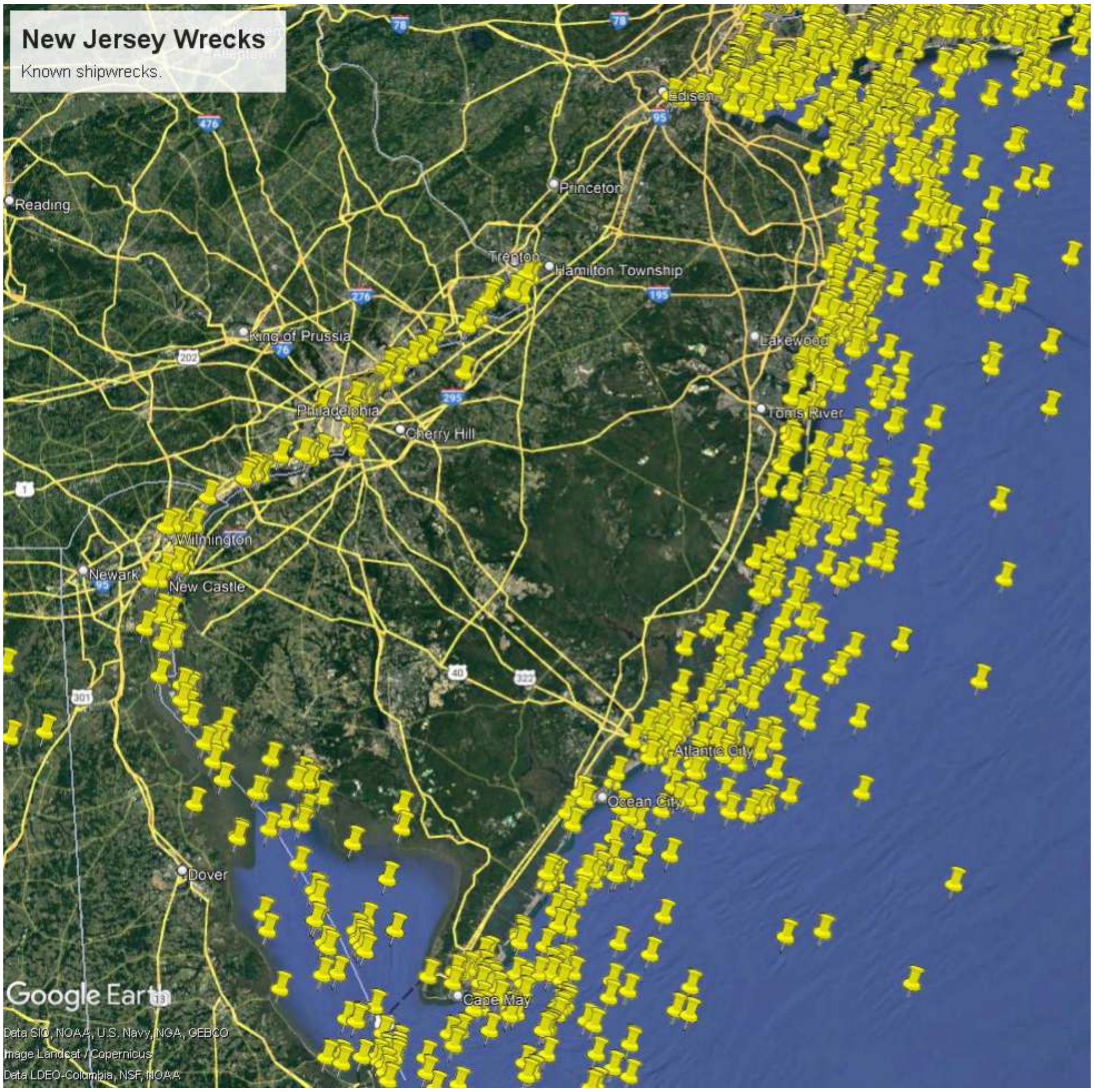

Figure 1. NOAA AWOIS (Automated Wreck and Obstruction Information System) map of charted shipwrecks along the New Jersey coast. Map created from public domain NOAA data superimposed on a basemap from Google Earth Pro by the author.

3.3 The Malta

Figure 2. Image depicting the *Malta* as the *Queen of the South* and with the original steam engine. Image rights purchased from Wrecksite.eu.

The iron-hulled full-rigged ship *Malta*, 243 feet long and weighing 1,611 tons, was built in London, England, in 1852, and sailed under the previous names *Milford Haven* and *Queen of the South* (New Jersey Maritime Museum 2021). Originally constructed as a coal-fired steamship, the *Malta* had the engine removed and was converted to all sail. On November 24, 1885, carrying a cargo of empty barrels, the *Malta* was driven aground in Belmar, off the current Ninth Ave, in a storm (New Jersey Maritime Museum 2021) (Galiano 2022). Through the work of the U.S. Life-Saving Service stations of Shark River, Squan Beach and Spring Lake, twenty-three of the twenty-four crewmen were saved (New Jersey Maritime Museum 2021). Portions of the *Malta* are currently visible at low tide, with the majority of the hull buried in the sand. This site provided an opportunity to fly an iron-hulled sailing vessel in close proximity to the shore, existing in both a buried and submerged state.

3.4 The Rjukan

The wooden-hulled, full-rigged ship *Rjukan*, 184 feet long and weighing 960 tons, was built in Boston, Massachusetts in 1856 (New Jersey Maritime Museum 2022). The *Rjukan* was sailing under a Norwegian flag from London, England to New York City carrying no cargo when she grounded and was lost off Bradley Beach in the area of Park Place Avenue on December 26, 1876 (New Jersey Maritime Museum 2022). By 0630 in the morning and shortly after running aground in thick fog, the vessel was swung broadside to the waves and had lost all her masts, eventually breaking in in half and completely submerging by the afternoon (Gentile 2000:153-154). The crew of twenty was saved by crews from the Shark River Life Saving Station (New Jersey Maritime Museum 2022). Diver reports state that the remains were fairly prominent several decades ago and consist of hull components, ballast, and one anchor. At the time of data collection, the vessel was covered in several feet of sand with no visible wreckage protruding from the bottom. The *Rjukan* presented an opportunity to fly a wooden-hulled vessel in shallow water, with a possible anchor magnetometer target.

3.5 The Sindia

Figure 3. Image depicting the *Sindia* aground. Reproduced with permission of Anthony Galiano, njscuba.net

The steel-hulled, four-masted bark *Sindia*, 329 feet long and weighing 3,068 tons, was built in Belfast, Ireland in 1887 (New Jersey Maritime Museum 2022). Sailing from Kobe, Japan to New York, she was blown off course in the early hours of December 15, 1901 and grounded into the sand between 16th and 17th Streets in Ocean City, becoming filled with a mixture of sand and water within one day, cracking the hull and becoming a total loss (Allen 2008). Historic photos show that the ship has broken into multiple large pieces, including distinct separation of the bow and stern sections. The *Sindia* presented the opportunity to fly a large, steel-hulled ship buried approximately twenty feet deep in the sand.

The culmination of representative hull types in the three locations chosen for UAV flights allowed for sufficient data collection to test system capabilities without presenting bias to ship material or period of construction. Furthermore, by choosing sites that existed in multiple environments within the littoral zone, the real-world survey capabilities of the UAV were tested while providing quality data, proving the technological capabilities and limitations and the overall effectiveness of the system within the target environment.

Chapter 4: Methods and Data Collection

4.1 Technological Development

The development and advancement of unmanned aerial systems (UAS or drones) has allowed new opportunities to bridge the gap between ground and vessel-based monitoring systems and airborne remote sensing methods. Miniaturization of processing and sensor technologies, coupled with stable UAS platforms operating in the ten-meter above ground range, has allowed for the implementation of advanced remote sensing surveying for the detection of unexploded ordinance and other niche applications. The application of this technology to the maritime cultural landscape has the potential to deliver effective, precise, and low-cost remote sensing surveys to target areas and environments that normally preclude traditional survey methods, such as in the three locations identified in Chapter 3.

This project utilized the MAGPi ML-4 magnetometer for data collection. The MAGPi ML-4 was developed by White River Technologies by combining control electronics, data acquisition, synchronization and logging, auxiliary sensors, real-time processing, and magnetometers in one device (Schultz et al. 2021). To achieve these capabilities, the MAGPi ML-4 combines an atomic gradiometer array magnetometer, a vector magnetometer, an altimeter, an on-board RTK-GPS, and an inertial measurement unit (Schultz et al. 2021) (Foley et al., 2019). This is combined into a 135mm x 25mm x 32mm ruggedized carbon fiber tow bird, weighing approximately 1 kg (2.2 pounds), with an onboard four-hour battery power supply and locally stored and Wi-Fi/ radio telemetry accessible communications (Schultz et al. 2021). This magnetometer array is capable of detecting ferromagnetic material at ~1 picoTesla sensitivity

(Schultz et al. 2021). Data points were collected at a rate of two hundred samples per second for all survey locations.

The MAGPi ML-4 was suspended from a Matrice 600 Pro 6-rotor drone for aerial delivery over the survey sites (Figures 4 and 5). Weighing 10 kg with the capability of taking off with an additional 5.5 kg payload, the Matrice 600 Pro is capable of ascent rates of 8 meters/second, horizontal speed of 17.9 meter/second without wind, with a hover time of eighteen minutes with a full 5.5 kg payload (*Matrice 600 Pro - Product Information - DJI*, 2022). This multirotor system allows for completely pre-programmable flight over a predefined area utilizing a simple waypoint navigation system. Coupled with integrated flight stabilization, station keeping, altitude control, and precision line following, this UAS is able to effectively keep the MAGPi ML-4 over precise transects in a dynamic maritime environment, with horizontal precision of ±1.5 m (4.92 feet) and vertical precision of ±0.5 m (1.64 feet) (*Matrice 600 Pro - Product Information - DJI*, 2022). Magnetic noise from surrounding sources, including the UAS, power supply, controls, and avionics, is removed through continuous compensation software.

Figure 4. Matrice 600 Pro 6-rotor drone with MAGPi ML-4 on carbon fiber rod. The launching and landing zone for the drone is the tarp. Photo by the author.

Figure 5. Matrice 600 Pro 6-rotor drone with MAGPi ML-4 on carbon fiber rod in flight. Photo by the author.

4.2 Site Selection Criteria

A total of three sites were selected that represented multiple types of ship hull construction materials, specifically steel, iron, and wood, to accurately test the capabilities of the MAGPi ML-4 to detect a broad spectrum of wreck sites and cultural material commonly found in the archaeological record. Sites were evaluated based on three criteria for project specifications:

4.2.1 Criteria 1: Location

Survey sites were located within several hundred meters of shore, with preference given to sites located as close as possible to land. Towed submerged magnetometers have developed to be capable of providing accurate, deep water survey capabilities, and this thesis did not seek to determine the capabilities of aerial magnetometry in deep water. Due to the increasing depth, as the distance from shore increases, the ability for a magnetometer to detect ferromagnetic items from a cultural context significantly decreases from an aerial platform. Additionally, while the UAV platform has a range of over two miles, losing the platform and magnetometer over water would have been an irrecoverable and catastrophic loss. For platform safety, minimizing the distance over open water was paramount. The UAV had been programed to take off and return to a specific location. As such, all sites had an appropriate terrestrial landing zone. No flights were conducted from the deck of a vessel, although this would be plausible in theory.

4.2.2 Criteria 2: Previous Site Identification

Survey site locations were required to be known and documented. Prior investigation and documentation of material type (wooden hulled vessel with associated ferrous material, iron hulled vessels, and steel hulled vessels) allowed for precise collection criteria to be determined and allowed for predictive modeling of future search results. By only surveying previously identified sites, a significant amount of time was saved for initial data collection. Additionally, by comparing previous diver survey data to collected data, results were easily correlated to determine capabilities. Additional weight in site selection was given to sites where the history of the shipwreck was known.

4.2.3 Criteria 3: Legality of UAV Operations

All sites flown were done so following all applicable local, state, and federal laws and ordinances. All local town and city administrations were contacted for permissions to fly, and all local police departments were contacted both for permission and for notification purposes the day prior to flying. At the time of this project, all U.S. Department of the Interior locations (locally including properties under control of the United States National Park Service and United States Fish and Wildlife Service) were off-limits to drone flights.

4.3 Safety Considerations

No flights over individuals not engaged in the operation of the drone were conducted. Individuals assisting with the project restricted pedestrian access around the project area during flights, including over jetties and rock groins. Flights were postponed until surfers were out of the water in the project area. No avian wildlife was observed in the flight area before flights commenced, and no helicopters or aircraft were in the vicinity at the time of flights.

4.4 Pre-Flight Operations

Specifications on shipwreck site locations were developed after consulting historical accounts, historical news publications, documents, logs, historic aerial photographs, and most importantly, diver reports and sketches of wreck sites. Google Earth Pro was utilized to draw initial 150-meter x 60-meter plots to develop KMZ (Keyhole Markup Language) files of 3D geographic coordinates of flight areas, which were directly inputted into flight control software to develop flightpath parameters. Upon field examination of flight locations, the flight paths were edited, increasing the total flight area to ensure each wreck was covered with enough of a buffer to provide background magnetometer readings, given potential discrepancies in site locations. Edits to flight paths were created directly on the touch screen of the Matrice 600 Pro controller.

Prior to flying, computers and supporting electronic equipment were set up on a relatively flat surface on the beach. A three meter by three meter (ten-foot by ten-foot) tarp was placed on the beach, drawn taught, and secured utilizing eight sand anchors. This tarp allowed for a controlled take-off and landing location and prevented the rotors of the Matrice 600 Pro from causing sand to adversely impact the mechanical components of the drone. Take off and landings were conducted manually, with the drone proceeding to the predefined flight path after takeoff. Once the flight was concluded, the Matrice 600 Pro was returned to a hover over the tarp. The MAGPi ML-4 was connected to the bottom of the Matrice 600 Pro with a controller switch operated quick release, allowing for the magnetometer assembly to be jettisoned prior to landing, preventing it from becoming an obstruction during the landing process.

An initial flight was conducted using the Matrice 600 Pro and no payload, to ensure flight operations. The air temperature at the time was 60 degrees Fahrenheit, with winds from the west at 16-19 km/hour (10-12 mph). The Matrice 600 Pro followed a pre-defined grid of 10-meter wide transects at 10 meters altitude, flown at 4 meters/second. A compass error code was received upon landing, which was corrected by powering the Matrice 600 Pro off and back on prior to the next flight.

4.5 Site Specific Flight Operations

4.5.1 The *Malta*

Upon viewing the site, the previously created flightpath was edited and expanded, bringing the area covered to eight transects at 110 meters in length each, and removing flights over a nearby rock jetty with fishermen on it for safety reasons. The area covered was expanded partially to ensure the entire wreck was included in the survey. While historic photos and statements described and showed the shipwreck as extending towards the beach from the exposed sternpost to the southwest, a surfer interviewed on location at the time of the survey described a strange set of ripples and wave breaks to the northeast, and thought the wreck could extend the opposite direction, away from shore. Weather conditions were a temperature of 62 degrees Fahrenheit, with winds from the west at 16-19 km/hour (10-12 mph) (Figure 6). As the Malta consists of the remains of the iron hull, the flight was conducted with transects spaced at 10 meters wide, at 10 meters altitude, at a speed of 4 meters/ second. The total distance covered during the flight was approximately 0.88 km in approximately three minutes and forty seconds.

Figure 6. *Malta* flight area, camera facing northeast. Photo by the author.

4.5.2 The *Rjukan*

Upon viewing the site and reviewing the hull material and potential remains on location (anchor to the northeast of the main hull), a flightpath was developed measuring 150m x 100m, including the edge of a large rock jetty/groin. Jetties and groins in the area were known to potentially contain large amounts of metal. The flight grid was developed to ensure total coverage of the wreck location, generated from diver sketches. Air temperature at the time of the flight was 65 degrees Fahrenheit, with winds from the west at 16-24 km/hour (10-15 mph) (Figure 7). Given the wooden nature of the wreck and assumed low quantity of ferromagnetic materials, the flight was conducted with transects spaced at 10 meters, at 8 meters altitude, at a speed of 4 meters/second. The total distance covered during the flight was 1.6 km in six minutes and forty seconds.

Figure 7. *Rjukan* flight area, camera facing northeast. Photo by the author.

4.5.3 The *Sindia*

Presenting a large target potentially broken into multiple sections and buried approximately 6.1 meters (20 feet) under sand, a large grid was proposed for the test flight at a higher altitude to prevent oversaturation of the magnetometer. By the time the site was accessed, air temperatures had dropped to 50 degrees Fahrenheit, with winds from the south sustained at 25.7-32.2 km/hour (16-20 mph), gusting to 40-48 km/hour (25-30 mph) at ground level (Figure 8). This was pushing the safety threshold and flight comfort level of the operator, with anticipated higher wind gusts at altitude. It was decided to hand survey the location of the Sindia with the MAGPi ML-4 to gather data. The MAGPi ML-4 was secured to a 2-meter (6.56 foot) carbon-fiber pole and walked in rough transects over the wreck site by a graduate student wearing no metal objects, including components of pants and shoes (Figures 9 and 10). Seven transects were walked, each approximately 320 meters in length. The total distance covered was approximately 2240 meters.

Figure 8. *Sindia* survey area, camera facing northeast. Photo by the author.

Figure 9. Handheld magnetometer data collection for the *Sindia* carried by an undergraduate student from West Chester University. Photo by the author.

Figure 10. Handheld magnetometer data collection transects for the *Sindia* carried by an undergraduate student from West Chester University. Photo by the author.

4.6 Additional Data Sources

In order to fully understand the detection capabilities of the MAGPi ML-4 UAV platform, data tables were created of common materials found on archaeologically researched and excavated historic shipwrecks, both by the author and other professionals. All measurement types listed below can be found in the following tables in Chapter 5.

Size measurements of iron ship fittings from the *Woodland Beach Shipwreck* in Delaware were taken by hand by the author, along with weights using an AMW-Bench digital scale series version 2.0 (Table 1). Additional measurements of iron fittings (pins, knees, bolts, and pintle pins) were taken from technical reports by the U.S. Army Corps of Engineers investigation of the *Barnegat Inlet Shipwreck* (James, Jr. & Gifford, 2015:100-119), the *Martinak Boat Wreck* (Thompson, 2005:7-15), the *Seal Cove Shipwreck* (Price et al., 2014:138), the *Roosevelt Inlet Shipwreck* (Southeastern Archaeological Research, Inc., 2010:260), the *Queen Anne's Revenge* (North Carolina Department of Natural and Cultural Resources, 2021), and work by Vanhorn (2004:75-77, 110, 114-115).

Measurements of armaments typically found on shipwrecks were taken from technical reports by Meide (2016), the *Queen Anne's Revenge*, the *Phinney Site*, and estimates from produced data tables based on traditional cannon production standards (Collins, n.d.). While ships in the historic period carried a multitude of different cannon sizes, the smallest cannon typically carried and found in the archaeological record are swivel guns (Hunter 2004:74), 4-pounder cannon (Hunter 2004:74), 6-pounder cannon (Vanhorn 2004:72), and 9-pounder carronade (Meide 2016:144). While larger cannon were typically carried, in order establish the minimum detection capabilities of the drone, the smallest artillery pieces by length, diameter, and weight have been chosen to establish an effective baseline (Table 2). As a compliment to the armament listed above, a three and four-pound cannonball was analyzed, with data from (Collins, n.d.) (Table 3).

Ship anchor weights have also been included since an anchor was encountered on the Rjukan shipwreck. Anchors were chosen based on the smallest weight for the smallest tonnage vessel recorded by the British (Table 4). While many anchors are substantially larger, this data covered some of the smallest oceangoing and coastal vessels that appear in the archaeological record.

Effective modeling of the minimum detection distance of iron hull components by the MAGPi ML-4 also depended on the relative densities and spatial relationship of iron ship fittings in wooden hull material. In order to test this distribution, data relating to relative densities and distances between fittings was taken from archaeological investigations of the *Biscayne Wreck* (Bright & Brown, 2013:4-11), *Seal Cove Shipwreck*, and *Barnegat Inlet Shipwreck* (Table 6).

The combination of precise data collection from the locations described above, coupled with the generation of post collection processed map overlays from project flights as showing the following chapters, allows for rapid determination of the ability for the MAGPi ML-4 UAV setup to identify cultural material effectively and accurately within the maritime cultural landscape. The results of data collection, displayed as two and three-dimensional grid maps in the following chapter, provide the raw data and the foundation for advanced interpretation of information related to the ability of the MAGPi ML4 to identify variations in the Earth's magnetic field due to buried archaeological resources.

Chapter 5: Results

5.1 Aerial Magnetometer Surveys

Data from UAV flights over the three target locations was processed by Dr. Greg Schultz of White River Technologies. 3D profiles of each anomaly were created, with the anomalous field deviation in nanotesla (nT) displayed in relation to the northing and easting of each flight transect. A minimum of one two-dimensional grid displaying deviations of up to ± 30 nT for each location was created, with some locations receiving additional grids as described below. Finally, KML files were created for each two-dimensional grid for ease of display in Google Earth Pro.

5.1.1 The *Malta*

The iron-hulled *Malta* was the first location flown. Eight transects were flown in an attempt to cover the area of the wreck in its entirety with a buffer around the perimeter of the site. A large dipole anomaly with a deviation of ± 400 nT was recorded in the flight location, oriented east-northeast to west-southwest (Figure 11). Due to the strength of the magnetic deviation, a single 30 nT two-dimensional map was created for georeferencing purposes (Figure 12).

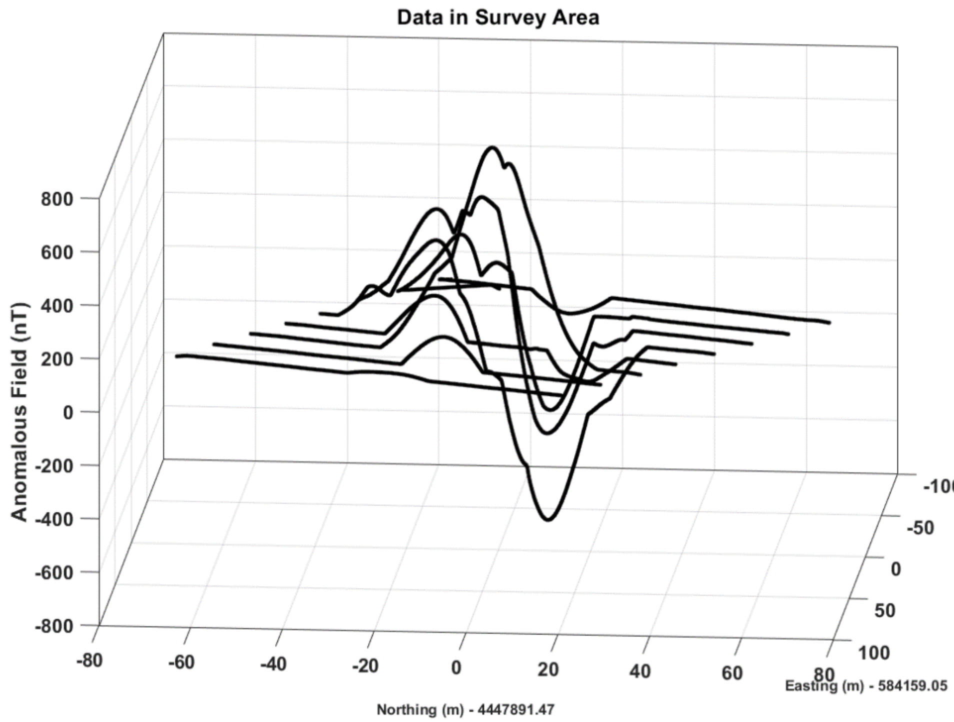

Figure 11. *Malta* 3D magnetometer data profile produced by Dr. Greg Schultz.

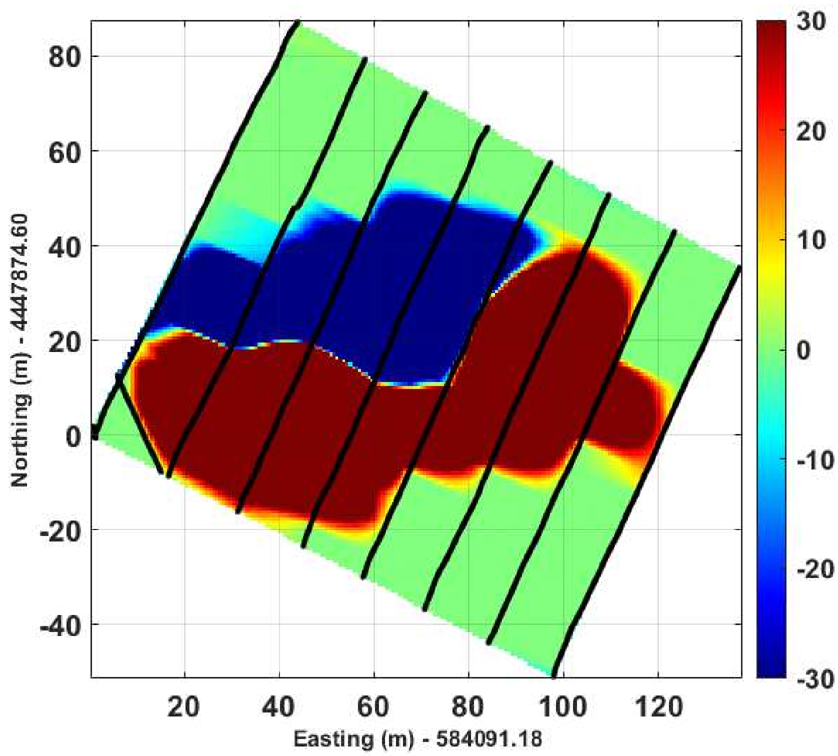

Figure 12. *Malta* 2D 30 nT scale grid produced by Dr. Greg Schultz.

5.1.2 The *Rjukan*

The wooden-hulled *Rjukan* was the second location flown. Ten transects were flown in an attempt to cover the area of the wreck in its entirety with a buffer around the perimeter of the site. A single dipole anomaly along the eastern edge of the flight area was identified, with a deviation of ± 8 nT, while a large anomaly with a deviation of > -30 nT was observed along the southern edge. Three ± 2-4 nT dipoles presented along the western and northwestern edge of the flight area (Figure 13). Three two-dimensional maps were created, one with a 5 nT grid (Figure 14), one with a 10 nT grid (Figure 15), and one with a 30 nT grid (Figure 16).

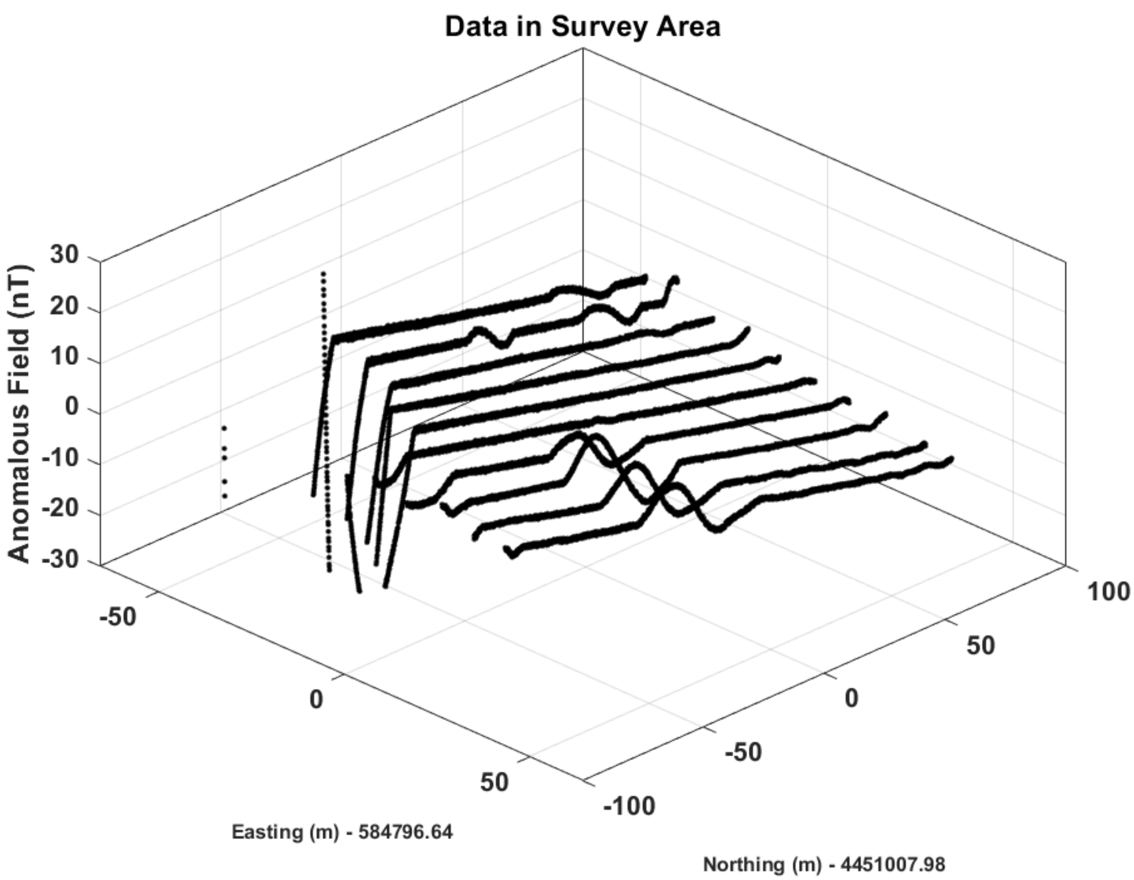

Figure 13. *Rjukan* 3D magnetometer data profile produced by Dr. Greg Schultz.

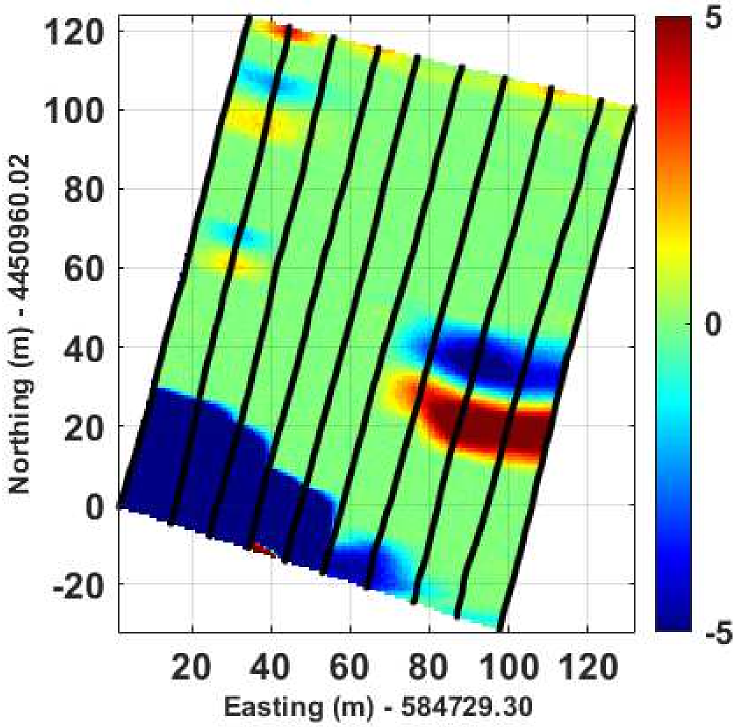

Figure 14. *Rjukan* 2D 5 nT scale grid produced by Dr. Greg Schultz.

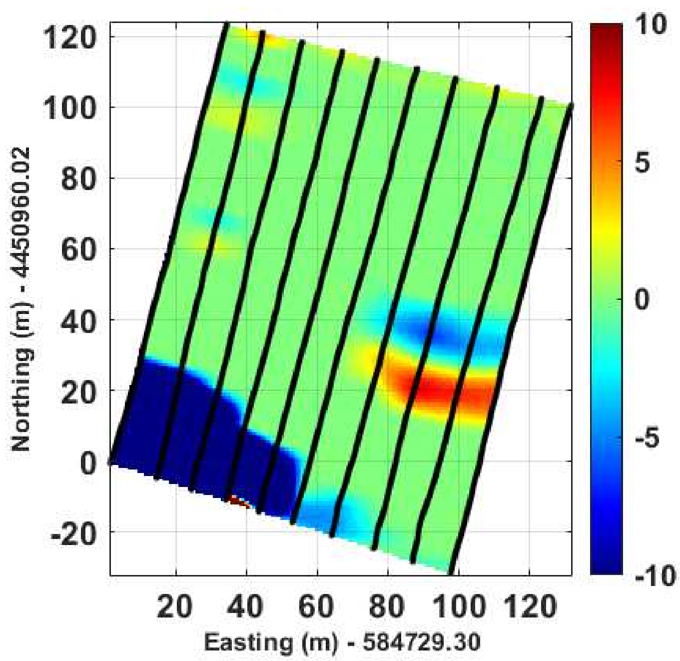

Figure 15. *Rjukan* 2D 10 nT scale grid produced by Dr. Greg Schultz.

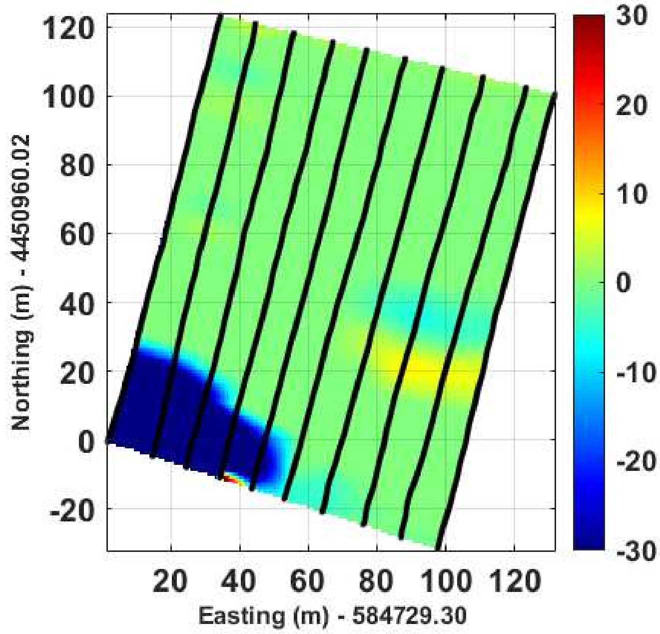

Figure 16. *Rjukan* 2D 30 nT scale grid produced by Dr. Greg Schultz.

5.1.3 The *Sindia*

The final location to be flown was the steel-hulled *Sindia.* Due to weather conditions, eight transects were walked while holding the magnetometer mounted on an extended carbon-fiber pole (Figures 9 and 10) in an attempt to cover the area of the wreck in its entirety with a buffer around the perimeter of the site. Multiple large dipole anomalies were identified throughout the survey area, with the strongest concentration of four distinct areas with deviations of ±300-500 nT in the center and along the western edge of the survey area. Three additional areas were identified to the north of the strongest concentrations, with two of these anomalies completely bisecting the survey area with a deviation of < ± 150 nT. A single dipole anomaly was identified to the south of the main concentration with a deviation of < ± 100 nT (Figure 17). Three two-dimensional maps were created, one with a 10 nT grid (Figure 18), one with a 30 nT grid (Figure 19), and one with a 50 nT grid (Figure 20).

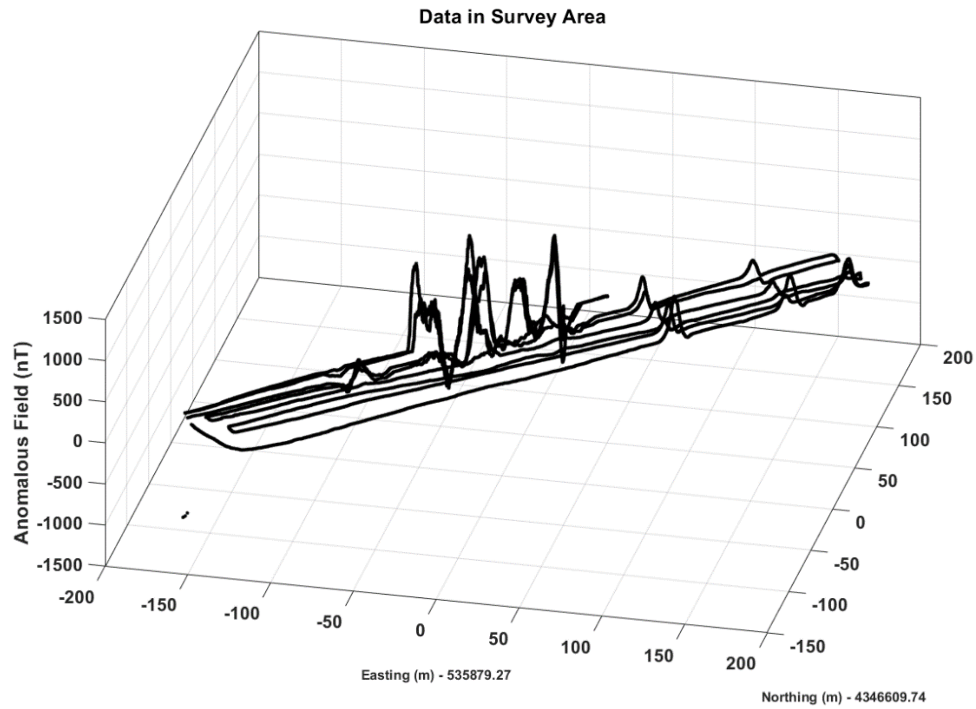

Figure 17. *Sindia* 3D magnetometer data profile produced by Dr. Greg Schultz.

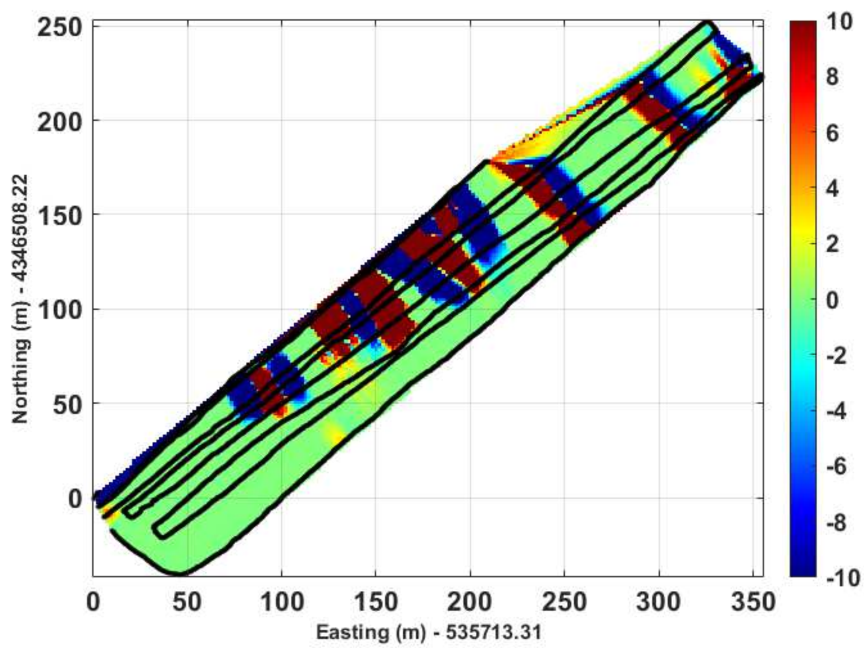

Figure 18. *Sindia* 2D 10 nT scale grid produced by Dr. Greg Schultz.

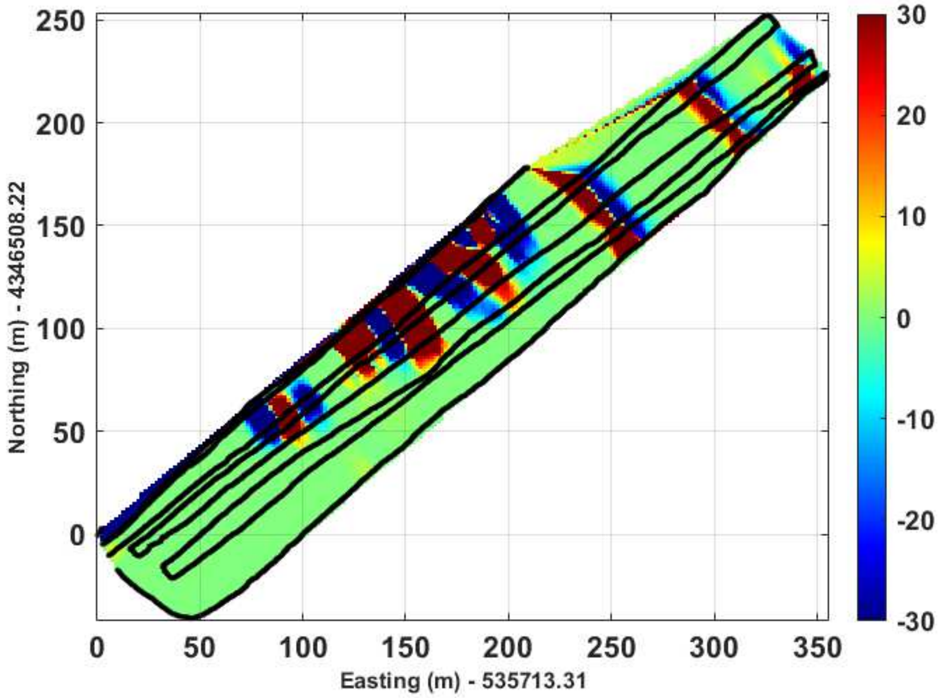

Figure 19. *Sindia* 2D 30 nT scale grid produced by Dr. Greg Schultz.

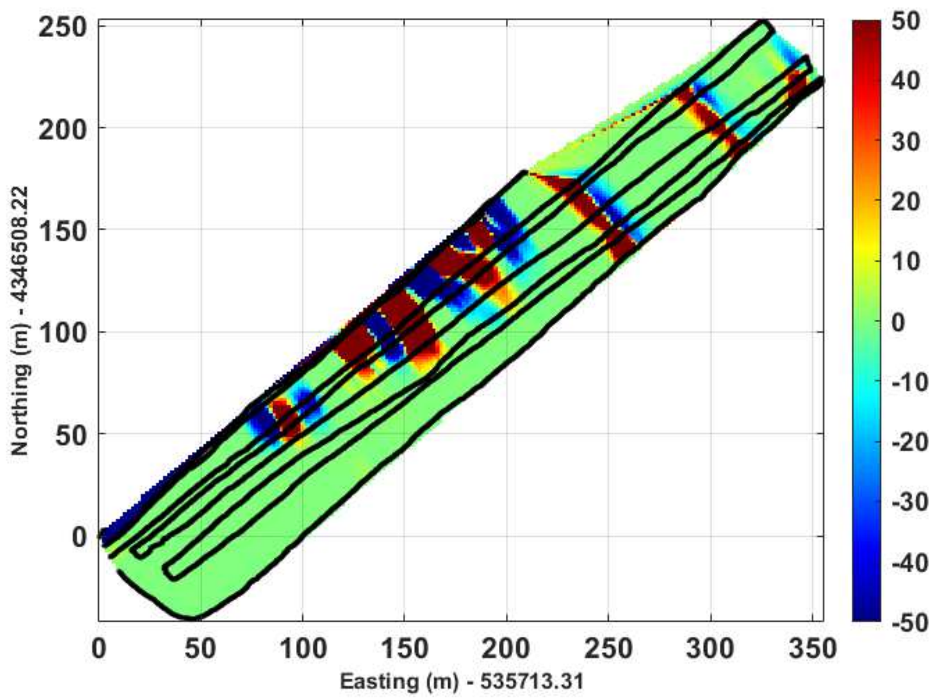

Figure 20. *Sindia* 2D 50 nT scale grid produced by Dr. Greg Schultz.

By overlaying the two-dimensional grids presented above onto georeferenced aerial photography, the accuracy of the data collection can be compared to historical accounts and records, allowing for interpretation of the magnetometer data and verification of system capabilities. Since all sites were flown where the location of the shipwreck was known and documented, the maps in the following chapter provided immediate verification of the data collection potential and capabilities of the system.

Chapter 6: Analysis

The raw data presented in Chapter 5 provides a framework for practical application and mapping to known cultural resources. While the raw data definitively shows the presence of ferromagnetic material within the flight locations, direct correlation of the data with known cultural resources is needed to demonstrate the validity of collected data to specifically identify archaeological resources. Only through proper interpretation can the magnetic signature of the abundance of non-contributing modern anthropogenic ferromagnetic material within the project area be compared to the target material of this thesis. The data collected generally conformed with the anticipated results expressed in the introduction of this thesis, with the exception of the lack of iron structural components on the *Rjukan* shipwreck, as described below.

6.1 The Malta

While the UAV and magnetometer system were being configured at the project location immediately prior to the flight, the iron sternpost of the *Malta* was observed breaking the surface of the water (Figure 21). A surfer was field interviewed to ascertain if he observed any strange wave breaks in the area of the wreck that could confirm the orientation of the wreck. The individual stated that, based on wave break and bottom composition, he felt that the wreck extended to the northeast, away from the shore and in the direction of the end of a nearby rock groin. This assumption is contraindicated by the reports of the *Malta* aground and the prevailing swell and vessel deposition on the coast. The *Malta* was reported to have been driven aground while carrying empty barrels, implying a strike more or less bow first onto the beach, presumably close to shore, due to a lower draft due to the decrease in displacement from the lighter cargo. Additionally, the fact that she went aground during a fierce storm with no record of any attempt to tow her free would imply that it would be extremely unlikely that the *Malta* is facing away from the beach.

Figure 21. The sternpost of the *Malta* visible in the lower left-central of the photo. Photo by the author.

The magnetometer data overlay of the 30 nT grid over the existing shoreline matches the observed location of the wreck precisely (Figure 22). The location of the visible sternpost is represented as the upper northeastern area of the magnetic anomaly, with the buried remains of the *Malta* extending to the southwest, extending to the edge of the survey area. The initial flight area was expanded before the data flight to attempt to include the entire vessel- had this not occurred, a significant portion of the vessel would have extended beyond the survey area. This orientation of the shipwreck validates the assumption of the orientation of the *Malta*, and is confirmed by referencing a photograph of the *Malta* breaking up in the surf several years after running aground (Figure 23). In this photo, the existing sternpost is visible to the far left, with the white breaking surf indicating that the image was taken facing east, with the *Malta* hard aground with her bow facing the beach.

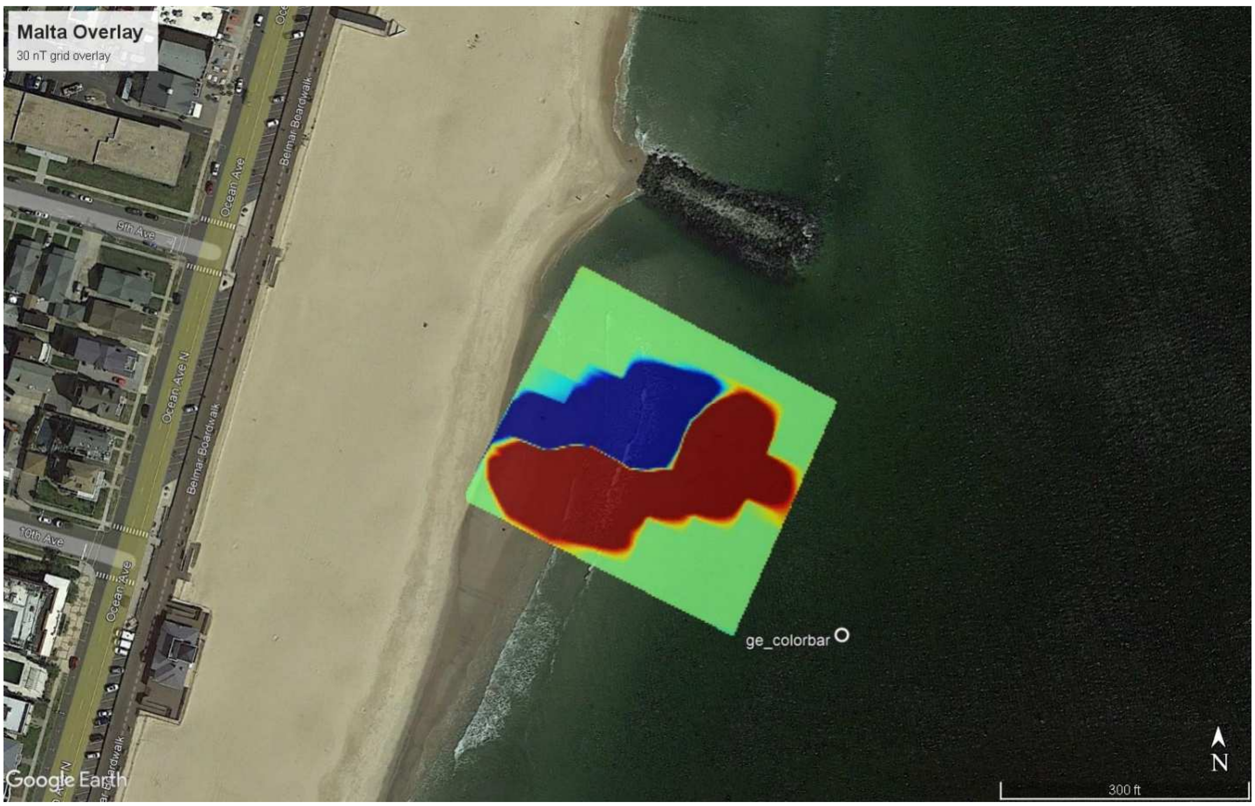

Figure 22. 30 nT map showing with dipole anomaly showing the location and orientation of the iron-hulled, full-rigged ship *Malta*. Overlay produced by the author using Googe Earth Pro and a georeferenced map produced by Dr. Greg Schultz.

The slight asymmetry of the magnetic anomaly, as seen above, may represent an uneven distribution of hull material, although the hull itself appears to remain in one contiguous piece.

The strength of the dipole has the potential to completely obscure any associated artifact scatter of a similar vessel.

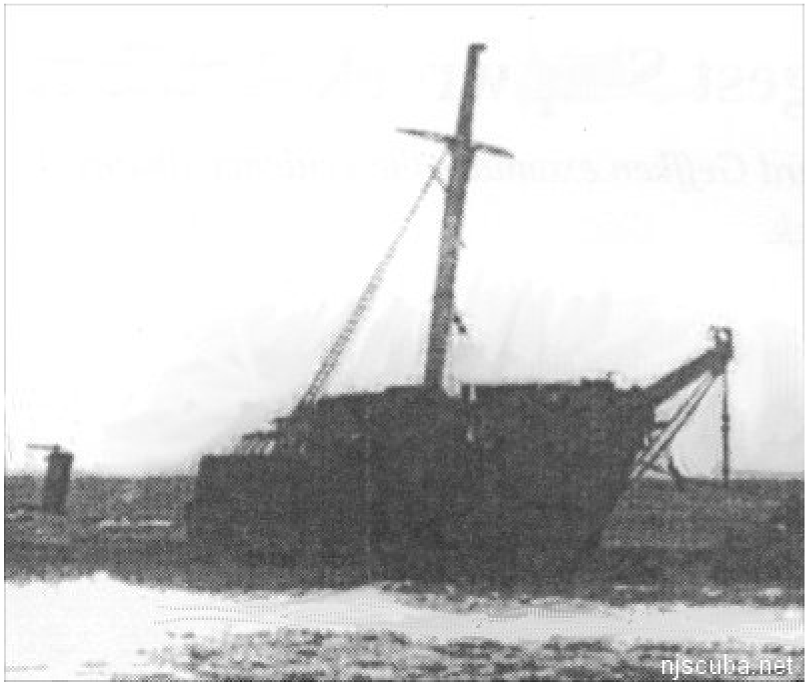

Figure 23. Image depicting the *Malta* breaking apart. The sternpost, still visible to this day, is the dark object protruding from the water in the lower left portion of the photo. Reproduced with permission of Anthony Galiano, njscuba.net

Additionally, photographs taken of the *Malta* during extremely low tides confirm the orientation of the shipwreck and the validity of the data interpretation (Figure 24).

Figure 24. Photo of the stern and ribs of the *Malta* during an extremely low tide, with camera facing west. Photo reproduced with permission from the Belmar Lifeguards.

The geophysical data produced by flying the *Malta* wreck site confirms that the MAGPi ML-4, when utilized as a payload from a UAV, can accurately detect the location and correct orientation of a contiguous, iron-hulled shipwreck that is buried in sand and submerged in the high energy surf zone.

6.2 The Rjukan

The *Rjukan* presented no visible components to assist with determination of the appropriate flight location, except for a single sketch map drawn by divers from 1993 (twenty-nine years before the date of the project). The expanded flight path was able to encompass a majority of the shipwreck per the sketch, including the large magnetic dipole (Figure 25).

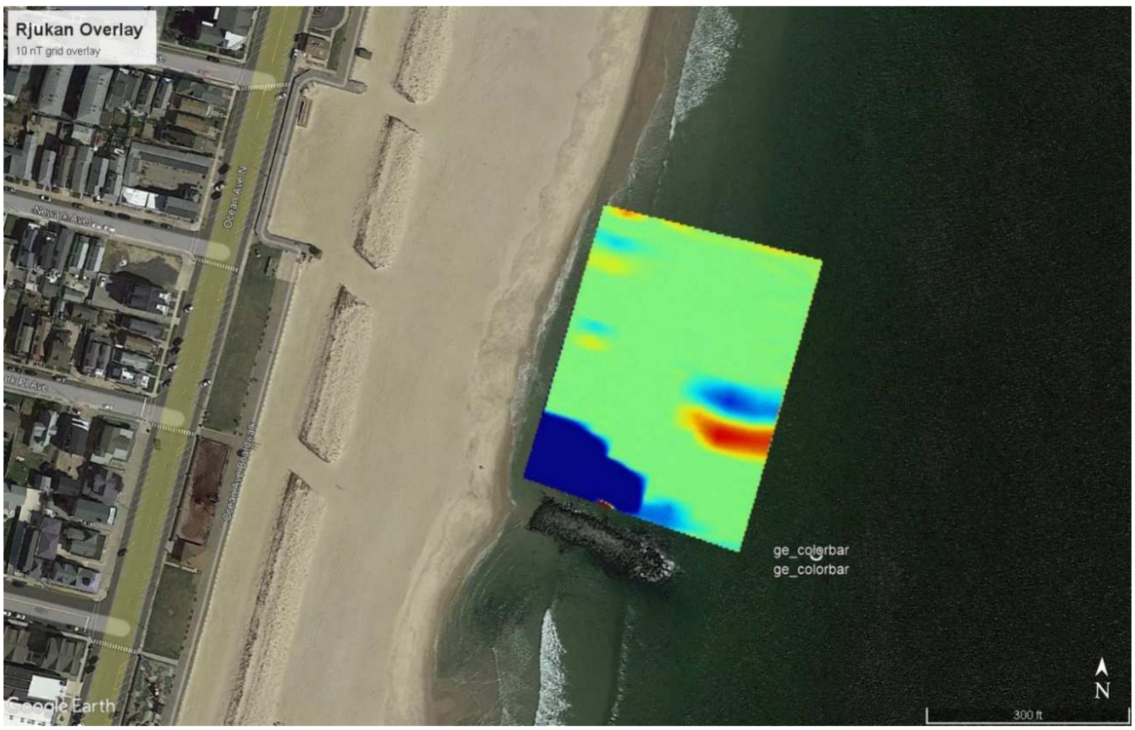

Figure 25. 10 nT map showing with dipole anomaly showing the location of the wooden-hulled *Rjukan*. Overlay produced by the author using Googe Earth Pro and a georeferenced map produced by Dr. Greg Schultz.

The simple dipole anomaly along the eastern edge of the survey area corresponds to the reported anchor on location. An image overlay was created in Google Earth Pro to show the approximate wreck location and orientation with the corresponding anchor (Berg 1993:59-60). No other magnetic anomalies were detected in association with the *Rjukan* hull remains. Divers report the presence of bronze spikes on the vessel and wooden treenails, representing a significant lack of ferromagnetic material and fasteners. The hull is reported to have broken into two distinct sections, each approximately 18 meters (60 feet) in length and separated by a distance of roughly 9 meters (30 feet), presenting an overall length of approximately 45.7 meters (150 feet) (Berg 1993:59-60). This overall length is not reflected in the magnetometer data, correlating the diver reports of non-ferromagnetic material on the *Rjukan* with the exception of the anchor. Only the iron anchor was detectable at an altitude of 8 meters. A strong negative magnetic anomaly was observed with a deviation of > -30 nT to the south and southwest of the flight area, correlating with iron components of the rock jetty. Had the *Rjukan* been oriented in a similar direction as the *Malta*, bow facing the shore, the negative magnetic anomaly of the jetty would have the potential to obscure or alter part of the remaining magnetic signature of the wreck. Smaller magnetic anomalies were detected to the western edge and northwestern corner of the flight area, representing outfall pipes from the local drainage system (Figure 26). While the data collected from the *Rjukan* demonstrates the capability of the MAGPi ML-4 to detect large iron ship components, it did not prove the capability to detect small fasteners associated with some wooden ships. Unfortunately, the fastener material was not known until after the survey had been completed.

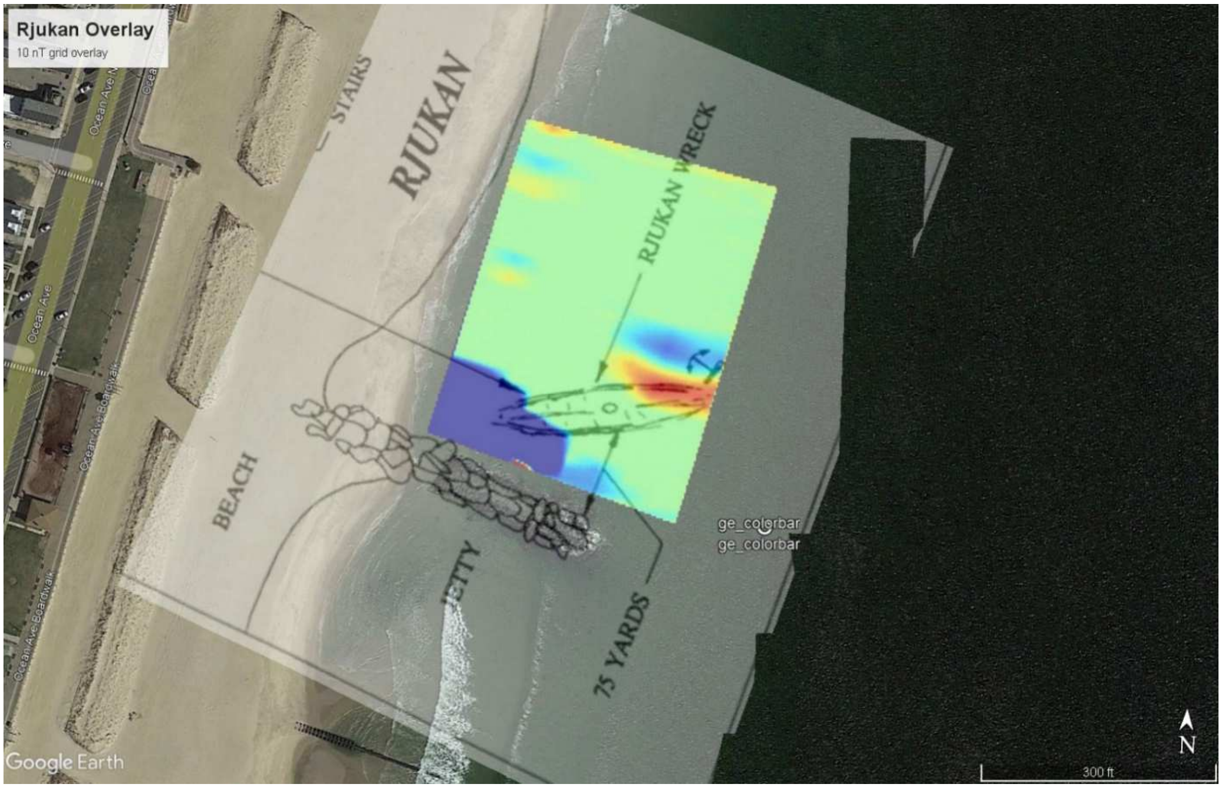

Figure 26. 10 nT map showing with dive sketch overlay showing the location of the *Rjukan* anchor in relation to the magnetic anomalies. Overlay produced by the author using Googe Earth Pro and a georeferenced map produced by Dr. Greg Schultz. Sketch map reproduced with permission from Gary Gentile (Gentile 2000:155).

6.3 The Sindia

The wreck location of the *Sindia* is well-documented, however the location itself presents as a flat, sandy beach. The last visible sighting of a significant portion of the hull material appears to have been following a storm in 1971. Historic photographs and postcards show that the hull had broken into at least three distinct portions by 1917, comprising the bow, a midship section with components of at least one mast, and the stern, including the rudder post. The rudder post has since been removed and is on display at the Ocean City Life-Saving Museum.

Historic aerial photographs from 1933 show the corresponding hull sections, with the bow, mast, and stern clearly visible (Figure 27).

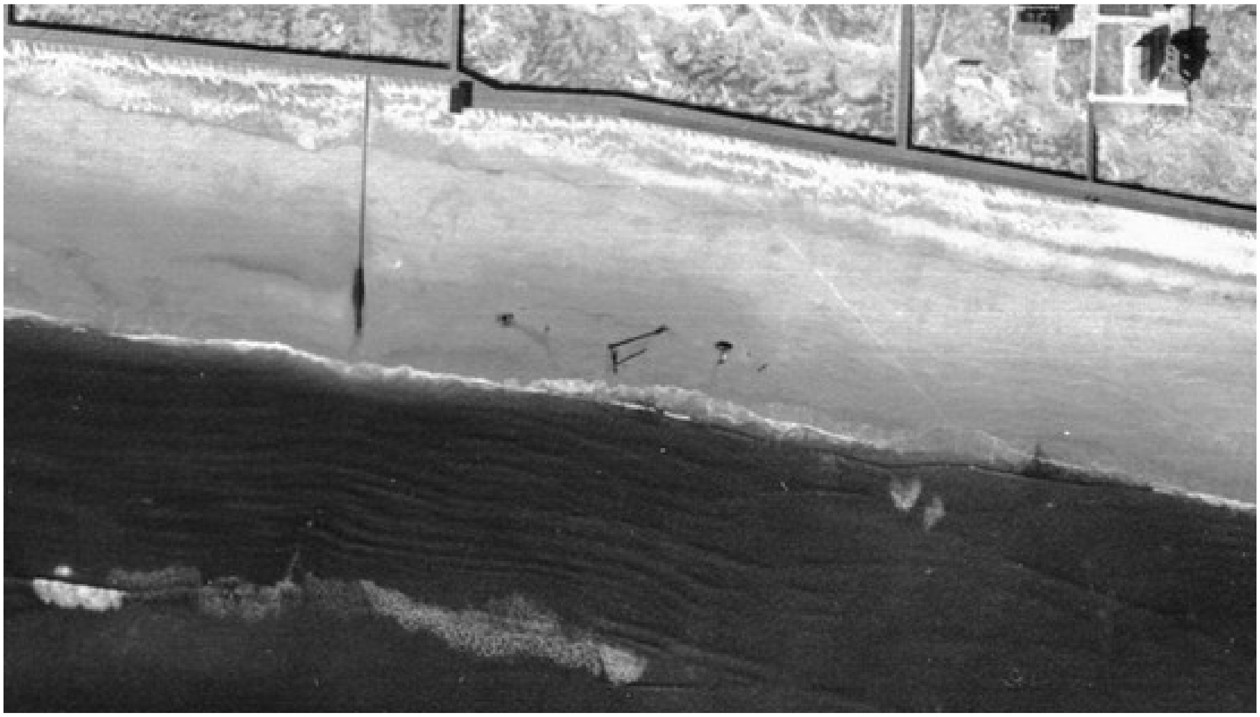

Figure 27. 1933 aerial photograph showing hull components of the *Sindia*. Accessed from https://rsm.usace.army.mil/shore/.

To correlate the data from the magnetometer survey, a simple overlay was created by manually georeferencing the 1933 historic aerial photograph and modern Google Earth Pro, showing the spatial relationship of the wreck location, outfall pipes, and the boardwalk. The 30 nT magnetometer data, saved as a .KML file, was then added into Google Earth, with opaqueness edited to show the background image of the historically visible *Sindia* shipwreck (Figure 28).

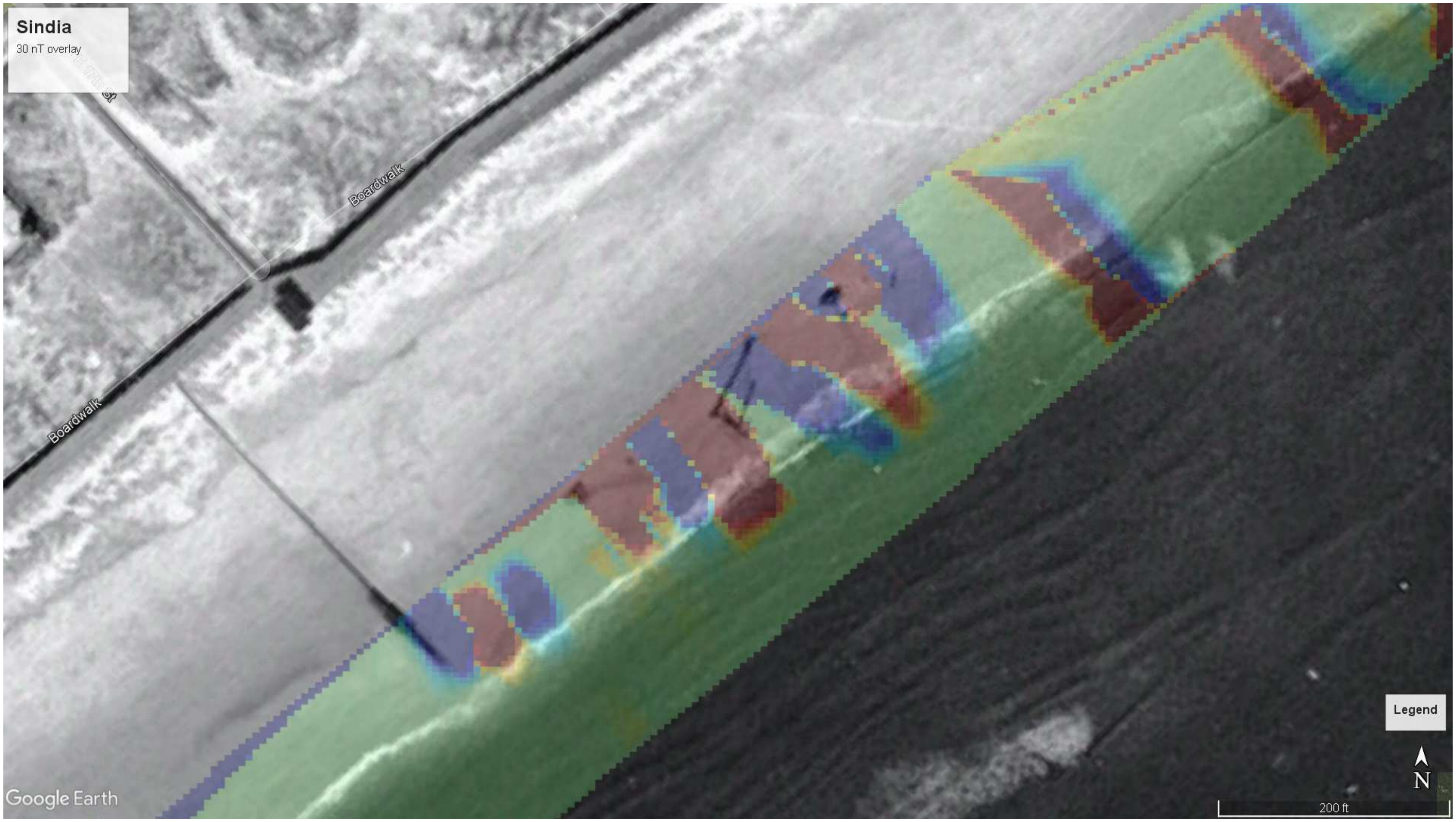

Figure 28. 30 nT magnetometer data overlay of georeferenced historic aerial photograph of the *Sindia* shipwreck. Data overlay produced by Dr. Greg Schultz, with historic aerial photograph accessed from https://rsm.usace.army.mil/shore/.

The strong dipoles in the center of the survey area correspond to the broken hull components of the *Sindia*, while the anomalies to the north and south of the central survey area appear to represent buried outfall pipes and other utilities in the area. Historic aerials form 1987 and 1995 show a large number of outfall and drainage pipes in this area, a common feature of many New Jersey coastal towns. The total saturation of the magnetometer was due to the low altitude of the survey, given weather conditions. The initial flight was designed to start at an altitude of 50 meters, given the size and anticipated mass of remaining hull material, but was reduced due to the need to conduct a pedestrian survey. Additionally, the survey was not positioned far enough to the west to incorporate the entirety of the wreck location, due to a protected dune area. Both of these factors would have been mitigated had a flight been possible. Even with these issues, the results of the pedestrian magnetometer survey of the *Sindia* demonstrate the capability of the magnetometer to accurately identify disarticulated hull material from a steel hull approximately 10 feet below ground surface. As with the *Malta*, the strength of the hull material magnetic anomaly has the possibility to completely obscure smaller artifacts.

6.4 Additional Ship Material

The three sites selected for magnetometer survey did not produce adequate data to make a determination on the ability of the MAGPi ML-4 to detect small ferromagnetic components of wooden-hulled shipwrecks. Due to limitations on availability of the magnetometer and UAV, predictive modeling based on tested magnetic detection algorithms from Bright et al. (2014:16-21) was used to determine detection capabilities of the utilized magnetometer system in the New Jersey maritime environment. Dr. Helmke and the author of this thesis held multiple meetings via Zoom to interpret the writings of Bright et al. (2014) to determine if a simple equation could be used to combine the known magnetic moment of archaeological iron with the mass of an object to determine the distance for detection at a certain nT strength. Following this, Dr. Helmke entered the modeling equation described below into an Excel spreadsheet to determine predicted minimum detection altitude from the objects identified and measured in Tables 1-4.

The formula utilized was:

$$r = \sqrt[3]{\frac{w\sigma}{\Delta\gamma}}$$

Where the distance from the sensor (r) is equal to the cube root of the object weight (w) in kilograms times the mass specific magnetic moment of the object (σ), expressed as $\frac{emu}{g}$, divided by the minimum detection magnetic anomaly value in nanotesla (Δγ), where Δ is the change and γ is the unit of measurement. In this formula, the minimum detection value (Δγ) was calculated as 1 nT. Although an object exhibiting a magnetic signature of less than 1 nT can be detected effectively in some situations, stronger magnetic signatures from adjacent shipwreck hull remains, cargo, or surrounding but noncontributing objects could obscure these small signatures, as was seen with the three survey areas of this project. This equation was developed directly from Bright et at. (2014:16-21). For calculation purposes of the magnetic moment of the object (σ), the value for pure iron was used with an archaeological material scaling factor developed by the National Park Service

Submerged Resources Center and provided to the author as an Excel spreadsheet (National Park Service n.d.). This measurement is a combination of the value of the magnetic field of the Earth at a given location at a given time and a scaling factor of 0.5 for the true magnetic value of archaeological iron when compared to the theoretical magnetic signature of true iron (Bright et al. 2014:61-62). This scaling factor was developed to account for changes in the composition of iron in archaeological settings, where magnetic signatures are influenced both positively and negatively by environmental factors, such as the site formation factors and chemical environment of submerged iron (Bright et al. 2014:I-4). Conversely, a larger scaling factor of 1 to 1.5 can be used for more recent shipwrecks or entire vessels (Bright et. al 2014:62).

6.4.1 Mass Specific Magnetic Moment

From data collected by Bright et. al (2014:62) and interpreted in the National Park Service Magnetic Moment Calculator, an average mass specific magnetic moment value (σ) of archaeological iron in New Jersey can be estimated at 12.01 $\frac{emu}{g}$ when subjected to an archaeological scaling value of 0.5. This may represent an ultra-conservative magnetic moment value, but for the purpose of survey planning, accounting for the absolute minimum value and detectability range may ensure that even the most ephemeral archaeological materials are detected. In their paper, Bright et al. recommends using conservative scaling factors to develop a worst-case scenario for testing purposes (2014:I-4).

The following tables were compiled by the author to determine hypothetical detection distances of iron components taken from investigations of actual shipwrecks to determine initial feasibility parameters for magnetometer flight surveys. The data from the *Woodland Beach Shipwreck* was collected by the author.

Hull Material	**Overall Length (cm)**	**Diameter (cm)**	**Weight (g)**	**Source**	**1 nT Hypothetical Detectability Distance**
Iron Pin	48	6.0	1187	Woodland Beach Wreck	2.42 meters (7.94 feet)
Iron Pin	24.3	7.5	633	Woodland Beach Wreck	1.97 meters (6.46 feet)
Iron Pin	54.4	9.2	1371	Woodland Beach Wreck	2.54 meters (8.33 feet)
Iron Pin	28.7	5.7	515	Woodland Beach Wreck	1.84 meters (6.04 feet)
Iron Pin	44.5	5.4	522	Woodland Beach Wreck	1.84 meters (6.04 feet)
Iron Pin	75.3	7.0	1559	Woodland Beach Wreck	2.66 meters (8.73 feet)
Iron Pin	52.3	6.7	1488	Woodland Beach Wreck	2.61 meters (8.56 feet)
Iron Pin	51.7	4.4	369.7	Woodland Beach Wreck	1.64 meters (5.38 feet)
Iron Pin	23.4	6.9	308.1	Woodland Beach Wreck	1.55 meters (5.09 feet)
Iron Pin	36.5	5.9	497.5	Woodland Beach Wreck	1.82 meters (5.97 feet)
Iron Pin	28.7	4.7	189.4	Woodland Beach Wreck	1.31 meters (4.30 feet)
Iron Pin	36.0	5.4	408.7	Woodland Beach Wreck	1.70 meters (5.58 feet)
Iron Pin	21.6	3.4	82.0	Woodland Beach Wreck	0.99 meters (3.25 feet)
Iron Pin	21.5	5.0	170.9	Woodland Beach Wreck	1.27 meters (4.17 feet)
Iron Pin	26.0	4.7	185.1	Woodland Beach Wreck	1.30 meters (4.27 feet)
Iron Pin	24.7	4.5	96.6	Woodland Beach Wreck	1.05 meters (3.44 feet)
Small Iron Pin	10.3	1.2	19.2	Woodland Beach Wreck	0.61 meters (2.00 feet)
Small Iron Pin	6.2	1.6	10.0	Woodland Beach Wreck	0.49 meters (1.61 feet)

Small Iron Pin	12.0	2.8	30.8	Woodland Beach Wreck	0.72 meters (2.36 feet)
Small Iron Pin	8.7	2.5	15.0	Woodland Beach Wreck	0.56 meters (1.84 feet)
Small Iron Pin	5.8	2.5	10.1	Woodland Beach Wreck	0.49 meters (1.61 feet)
Iron fastener	49.53	2.54	~1187	ACOE Barnegat Shipwreck (James and Gifford 2015: app. 1-2)	~2.42 meters (7.94 feet)
Iron fastener	76.2	3.81	~1559	ACOE Barnegat Shipwreck (James and Gifford 2015: app. 1-2)	~2.66 meters (8.73 feet)
Iron nail	12.7	2.03	~30.8	ACOE Barnegat Shipwreck (James and Gifford 2015: app. 1-2)	~0.72 meters (2.36 feet)
Iron bolt	45.01	2.01	~522	Martinak Boat Wreck (Thompson (2005)	~1.84 meters (6.04 feet)
Iron bolt	11.43	1.91	~30.8	Seal Cove Shipwreck (Price et al. 2015)	~0.72 meters (2.36 feet)
Iron bolt	24.13	1.91	~96.6	Seal Cove Shipwreck (Price et al. 2015)	~1.05 meters (3.44 feet)
Pintle Pin	??	3.81	~1559	Queen Anne's Revenge (North Carolina Department of Natural and Cultural Resources 2021)	~2.66 meters (8.73 feet)
Iron Pin	??	2.54	~10.1	Roosevelt Inlet Wreck (Southeastern Archaeological Research 2010)	~0.49 meters (1.61 feet)

Table 1. Ship fitting measurements for magnetic detectability determination.

Cannon Type	Overall Length (cm)	Muzzle Diameter (cm)	Weight (kg)	Weight (lb)	Source	1 nT Hypothetical Detectability Distance
4-pound cannon			1270		Bright et. al (2014)	24.80 meters (81.36 feet)
4-pounder cannon	154.4	24.0	426.4	940.05	Meide (2016)	17.24 meters (56.56 feet)
9-pounder carronade	101.0	15.0	199.6	440.04	Meide (2016)	13.38 meters (43.90 feet)
6-pounder cannon	182.88	Unknown	838	1850	McConnell (1988:88)	21.59 meters (70.83 feet)
4-pounder cannon	167.64 (appx)	13.97 (appx)	346.09	763.0	Queen Anne's Revenge (North Carolina Department of Natural and Cultural Resources 2021)	16.08 meters (52.76 feet)
1-pounder gun	121.92 (appx)	10.13 (appx)	138.35 (appx)	305 (appx)	Queen Anne's Revenge (North Carolina Department of Natural and Cultural Resources 2021)	11.84 meters (34.85 feet)
½-pounder gun	104.14 (appx)	9.32 (appx)	90.26 (appx)	199 (appx)	Queen Anne's Revenge (North Carolina Department of Natural and Cultural Resources 2021)	10.27 meters (22.36 feet)

Table 2. Ship armament measurements for magnetic detectability determination.

Ammunition	Poundage	Weight (kg)	Diameter (cm/in)	Diameter (in)	1 nT Hypothetical Detectability Distance
Cannon Ball	3	1.36	6.35	2.5	2.54 meters (8.33 feet)
Cannon Ball	4	1.81	7.75	3.05	2.79 meters (9.15 feet)

Table 3. Ship ammunition measurements for magnetic detectability determination from Collins (n.d.)

Ship Type	Hundredweight	Weight (kg)	1 nT Hypothetical Detectability Distance
Brig, 200 Tons	10	508.0	18.27 meters (59.94 feet)
Sloop, 200 Tons	3	152.4	12.23 meters (40.12 feet)
Sloop, 200 Tons	6	304.8	15.41 meters (50.56 feet)
Sloop, 200 Tons	15	762.0	20.92 meters (68.64 feet)
14 Gun, 300 Tons	3 Ton, 2 Qr	177.8	12.88 meters (42.26 feet)

Table 4. Ship anchor weights from Historic Naval Ships Association (2022).

6.4.2 Corrected Maximum Detection Range

While this calculation shows the absolute minimum detection range, it should be noted that a drone mounted, pedestrian, or towed array magnetometer will only detect the object at this distance if the object is in line with the survey transect. In order to effectively model what is hypothetically detectable during surveys, the Pythagorean theorem must be applied to determine the actual maximum potential distance of the target from the magnetometer, if the object were to exist at the maximum depth in the middle of the transect interval. To do so effectively, three altitudes for surveying were chosen: 10 meters (32.8 feet), 5 meters (16.4 feet), and 3 meters (9.8 feet). While it is easy to correlate this distance to altitude, that comparison is deceiving. The distance variable correlates to any combination of height above water or land surface, depth of water, and depth of buried material. For example, the 10-meter altitude flight of the *Malta* during this project only relates to the height of the UAV above the surface water based on the onboard barometric altitude control. It did not reflect variations in the wave conditions, nor did the 10-meter distance account for the several feet of water over the *Malta*, or the depth of the sand. Furthermore, the magnetometer itself was not flown at 10 meters, as it extended on a carbon fiber pole below the UAV. All these variables must be accounted for during pre-flight planning based on anticipated weather conditions, sea state, terrain, and depth of water and buried materials.

6.4.3 Vertical Distance and Transect Interval

The 10-meter sensor height over the anticipated target depth appears to be a good distance for platform safety over the surf zone. In an area of water depth approaching 3 meters and a vessel buried 1.5 meters in the sand, a 10-meter distance would still allow for an approximately 5.2 meter safety zone between water surface and the sensor. 1-to-1.8 meter (3-to-6-foot) waves would reduce this but still allow for a 3 meter safety buffer. Waves higher than 1.8 meters (5.9 feet) may be the result of strong wind conditions, which would potentially negate the ability for the UAV to fly a target zone effectively and safely. The 10-meter distance is also appropriate for sites deeply buried under accumulated beach sand, such as was seen with the *Sindia*. However, the significant distance between sensor and target precludes anything but the largest magnetic objects from being detected. A 5-meter distance is plausible for use over calm ocean conditions in shallow water, back bay, and estuary conditions with significant accumulation of debris and vegetation precluding vessel or pedestrian surveys, or over a shallow depth beach and dune area. The 3-meter distance is plausible for use over shallow estuary, tidal river and back bay waters and controlled environments where small ferromagnetic archaeological remains may exist in environmental conditions not conducive to alternative survey methods.

The transect interval should also be discussed and chosen appropriately, based on the anticipated nature of cultural material in the project area. While the 10-meter transect interval was utilized and correctly identified large ferromagnetic objects in this project (two vessel hull components and an anchor), a 5-meter transect interval may be more appropriate for small and disarticulated sites. By using the Pythagorean theorem ($a^2 + b^2 = c^2$), we can identify the length of the hypotenuse of the right triangle formed from the combination of sensor height and transect interval, giving us the maximum possible distance of detectable cultural material from the magnetometer (Table 5). The horizontal leg distance is equivalent to half the width of the transect, as the magnetometer should detect the object in the center at the same distance from either parallel survey transect. To get the minimum weight for 1 nT detection in Table 5, the same equation that was previously used in this thesis to solve for w that was used to solve for r, by adjusting the known variables:

$$r = \sqrt[3]{\frac{w\sigma}{\Delta\gamma}}$$

Vertical Elevation of Sensor	**½ Transect Width**	**Maximum Distance Between Sensor and Target**	**Minimum Weight for 1 nT Detection**
10 meters (32.8 feet)	5 meters (16.4 feet)	11.18 meters (36.68 feet)	116.35 kg (256.52 lb.)
5 meter (16.4 feet)	5 meters (16.4 feet)	7.07 meters (23.19 feet)	29.42 kg (64.86 lb.)
3 meter (9.8 feet)	5 meters (16.4 feet)	5.83 meters (19.13 feet)	16.50 kg (36.38 lb.)
10 meters (32.8 feet)	2.5 meters (8.2 feet)	10.31 meters (33.83 feet)	91.25 kg (201.17 lb.)
5 meters (16.4 feet)	2.5 meters (8.2 feet)	5.59 meters (18.34 feet)	14.54 kg (32.06 lb.)
3 meters (9.8 feet)	2.5 meters (8.2 feet)	3.91 meters (12.83 feet)	4.98 kg (10.98 lb.)

Table 5. Determination of distance between target and magnetometer sensor at given flight and transect parameters.

With this information, a true determination of the detectability of the typical iron artifacts from Tables 1-4 can be made. This directly confirms the known physics behind detection ranges for magnetic anomalies when using magnetometers. The most important component affecting detectability is the distance (r) between the magnetometer sensor and the target. A rough estimate of this correlation is that detectability decreases by the inverse cube of the distance. Even large magnetic targets can be impossible to detect at moderate distances. It should also be understood that the sensitivity of a magnetometer does not change the actual magnetic signature of an iron component in an archaeological context, which is based on the mass and orientation of the object in relation to the strength and orientation of the magnetic field of the Earth. Instead, the magnetometer sensitivity only changes the ability to see this signature with greater clarity and precision, and to detect ever-smaller changes in the magnetic field.

Based on the calculations explained in this thesis and the synthesis of archaeological material, at a 10-meter sensor height with a 10-meter transect, only the anchors and armament with the exception of the ½ pound cannon would be detected on a shipwreck, with the same results at the 5-meter transect interval. Based on this data, no single hull pins would be detected. A 5-meter sensor height with a 10-meter transect and a 5-meter sensor height with a 5-meter transect would detect all anchors and all armament. Finally, both 3-meter sensor flights at 10- and 5-meter intervals would still fail to detect individual iron pins and hull fasteners.

6.4.4 Superposition of Magnetic Fields

One very important aspect of magnetometry to understand before a final detectability conclusion can be made is the superposition of magnetic fields. As explained by Walker (2001), the total magnetic field is a sum of adjacent magnetic fields. This means that if multiple magnetic fields are present and close enough together, they will have a cumulative effect on detectability, either positive or negative. For this application, a general net positive cumulative effect was assumed. For example, in the context of the maritime archaeological landscape, while individual large iron pins are not detectable, multiple pins in close association, such as are found in surviving shipwreck hull timbers, can lead to increased detectability. If a hull timber contained iron bolts, each weighing 1 kg and spaced approximately 50 cm apart (density of two bolts per meter), and the magnetometer was positioned in the middle of the timber at a 3-meter vertical distance, their magnetic signature would be cumulative. The middle bolt would exhibit a signature of 0.45 nT. The bolts on both sides would decrease in field strength, but still be cumulative. A 10-meter-long timber would exhibit a total magnetic field signature of 4.66 nT, detectable at the 3-meter vertical distance UAV flight and would exhibit a detectable 1.39 nT at a 5-meter vertical distance UAV flight.

When superpositioning is applied to known iron component spacing of archaeological materials, a prediction can be made regarding the amount of linear feet of hull material required to exist at a location to hypothetically be detectable, based on the maximum distance from the magnetometer sensor based on transect interval. Using an iron pin with a conservative mass of 0.5 kg and comparing it to the intervals per meter of existing iron material recovered from the shipwrecks below (Table 6) gives a real-world detection distance value if the assumed piece of hull material containing the iron is 10 meters in length:

Material Type	**Iron Bolts Interval**	**Iron Fitting Mass**	**Source**	**Detectability**
Floor timbers to keel	2 bolts per meter	0.5 kg	Biscayne Shipwreck (Bright and Brown 2013)	Detectable at 3.91 m (1.26nT)

Keel to frame	1 bolt every 1.5 meters	0.5 kg	Seal Cove Shipwreck (Price et al. 2015)	Not detectable at 3 m
#1 Frame	6 bolts in 1 meter	0.5 kg	Barnegat Inlet Wreck (James and Gifford 2015)	Detectable at 7.07m (1.74nT)
#2 Frame	9 bolts in 1 meter	0.5 kg	Barnegat Inlet Wreck (James and Gifford 2015)	Detectable at 7.07m (2.62nT)

Table 6. Relative estimation of densities of ferromagnetic fasteners in surviving hull material.

Hull timbers with iron bolts are largely detectable at a distance of 3.91 meters, the maximum sensor to target distance from a flight consisting of 3-meter vertical distance from the target with 5-meter transects, while some denser compositions are detectable at 7.07 meters, the maximum sensor to target distance from a flight consisting of 3-meter vertical distance from the target with 10-meter transects. If the drone and magnetometer are flown in only one set of parallel transects, the chances of properly identifying cultural material significantly drops when compared to the incorporation of additional transects perpendicular to the first set. Incorporation of additional flights would decrease the maximum distance from the sensor to the target, thus diminishing the effects of the inverse square law in relation to magnetic detection.

Once again, it must be stated that the coefficient values used in this modeling represent the absolute minimum detection criteria. The archaeological scaling factor of 0.5 for the magnetic moment of archaeological iron represents very degraded iron artifacts with extremely low magnetic signatures. Of all the material studied by Bright et al., only one-third were represented by this low amount. One-third of the material in their study was at the scaling factor of 1, while the last third was at an increased scaling factor of 1.5 (2014:61). This would have a significant positive influence on the detectability range and capabilities of the MAGPi ML-4. Additionally, the ship armament used for predictive modeling represents the smallest guns carried on armed vessels encountered in the area, while the anchor weight records were taken from the smallest recorded vessels. Finally, the iron fasteners used do not include large iron ship knees, rigging material, windlasses, iron chain, or any other components, nor does the modeling include the signature of multiple structural elements together, each containing iron pins and fasteners. They were chosen to represent the smallest possible targets to develop the minimal magnetometer target thresholds.

The totality of the information presented in this chapter show that the system utilized not only provided an effective means of data collection of the three hull materials present within the survey areas, but that predictive modeling shows that the system is well suited for the detection of cultural materials containing relatively low amounts of ferromagnetic material, as can be found within the survey environment. While these materials were not present during this survey, additional research as described in the following chapter may help to fill in the data gaps and provide a more complete understanding of the capabilities and limitations of this system.

Chapter 7: Conclusion

7.1 Operational Capabilities

This project demonstrated that UAV-mounted delivery of remote sensing equipment in the high energy surf zone and beach environment may be one of the only viable and efficient options for successful surveys of shipwreck material within the challenging littoral zone, providing an effective means of conducting remote sensing surveys in the transitional area between terrestrial and underwater sites. Furthermore, it was demonstrated that this system can collect data to support site identification and preservation activities within rapidly changing coastal environments facing the challenges of sea level rise and degradation. With the exception of the lack of ferromagnetic material on the *Rjukan*, the detection results and distances at which they were obtained confirmed the expectations set out at the beginning of the thesis, providing a sufficient range of information in an applicable manner to support theoretical developments based on the relationship of shipwreck material and the broader maritime cultural landscape. This thesis confirmed that the Matrice 600 Pro 6-rotor drone and MAGPi ML-4 setup performs well under normal operating conditions in the maritime environment. While flying the locations of the *Malta* and *Rjukan*, the Matrice was able to precisely follow the pre-programmed flight transects without any issues and landed with significant battery reserves left, meaning a much larger area can be surveyed for project purposes. The altitude of the UAV for the *Malta* and *Rjukan*, 10 meters and 8 meters (32.8 and 26.2 feet) above the surface respectively, was a conservative number chosen due to the data collection flights being some of the first over open water. A lower altitude is possible for data collection in the future, while being cognizant of significant wave height being a limiting factor. With seas of approximately 1 meter (3.3 feet) in wave height and the carbon fiber pole and magnetometer assembly combination approximately 2 meters (6.6 feet) in length, flying at a future 5 meters above surface (16.4 foot) altitude will provide adequate data collection and flight control while maintaining a safe buffer altitude.

While the location of the *Sindia* was not flown, the data collected is still valid. The height of data collection from the magnetometer to the ground surface, approximately 3 meters, was within the flight capabilities of the Matrice over solid ground. Had wind conditions been more favorable for UAV flights, the altitude of data collection would have been similar, allowing for collection over the same area and the incorporation of transects from the protected dune areas.

UAV mounted data collection remains one of the best options for remote sensing in the areas flown during this project. The flight location of the *Malta* is entirely within the surf zone, where breaking waves occur during both low and high tide. Coupled with the sternpost being completely obscured at high tide, these conditions present an extreme hazard to any vessel operating in the area. Nearly the entire length of the shipwreck is buried under the sand, precluding effective survey and detection from side-scan sonar or diver. A search of NOAA published bathymetric data of the New Jersey coast indicates that this surf zone has not been surveyed via side-scan sonar, presumably due to the inability to maneuver a vessel in the surf zone.

The *Rjukan* survey location presents the same environmental challenges for traditional survey methods, meaning that UAV mounted survey methods present one of the only effective data collection and remote sensing survey platforms for this situation. While only the anchor was detected, this anomaly is buried under the sand, precluding detection from side scan sonar or diver investigation. Berg (1993:59-60) stated that the *Rjukan* was visible starting around 61 meters (200 feet) off the coast, while today the wreck is less than 30.5 meters (100 feet) from shore, sanded in due to beach replenishment work. A much lower survey altitude of 5 meters (16.4 feet) is plausible and potentially effective at detecting more archaeological material.

Although the *Sindia* exists beneath the sand, UAV surveys still provide an optimal delivery platform for remote sensing surveys. The Matrice incorporates onboard sensors, allowing for real-time altitude correcting to safely navigate over obstacles and terrain deviations, such as the sand dunes that precluded pedestrian survey during the data collection phase of this project. Without any significant features visible to narrow a survey area, use of a UAV in this environment allows for multiple low altitude transects over a broad area in a more effective and precise manner than pedestrian or aircraft surveys.

7.2 Detectability

All of the locations in this project contained some degree of ferromagnetic material, with the *Rjukan* presenting the lowest amount. Each site was detectable at a very conservative 8-to-10-meter flight altitude and 10-meter interval. Again, it should be noted that this altitude is not a reflection of the actual distance between the magnetometer sensor and the target. Even with the meter-long carbon fiber pole, the altitudes represent a distance above sea level, and do not include the variable distance from the sea surface to the bottom or the distance from the bottom to the buried target.

The data tables of detectability indicate that small iron components are easily missed in surveys, unless subjected to magnetic superpositioning. While some targets are individually not detectable at feasible altitudes and survey transect intervals, substantial hull remains have the possibility to be easily detectable at or above the one nanotesla threshold used for this paper. Additionally, when the archaeological scaling factor is increased, a positive effect on detectability occurs.

7.3 Limitations

Despite the advantages to the UAV setup utilized, several significant limitations exist. The first, and most significant, is the need for the shipwreck to contain ferromagnetic material. According to the data published from the New Jersey Maritime Museum, approximately seventy-three percent of known shipwrecks have hulls constructed of wood, and a lack of significant iron or steel materials would prevent detection. While predictive modeling can assist based on probable individual material components, there is currently no model or convention to determine the mass of ferromagnetic material within a wooden vessel based upon its size and dimensions (Bright et al. 2014:42). Had the anchor been salvaged or disarticulated from the hull material during the wrecking process, the *Rjukan* of this project would not have been detected.

Wooden vessels, therefore, present a unique challenge for a magnetometer survey. The percentage of shipwrecks in the New Jersey area that are composed of wood is most likely significantly higher, given the fact that roughly three thousand shipwrecks in the records have no hull material is listed, yet lay within a date range that strongly suggests a wooden construction. Some wooden vessels lost off New Jersey were armed and present a strong magnetometer target from the cannon and ammunition on board, such as the HMS *Fowey* in Biscayne National Park, which presented multiple magnetometer targets representing the armament that were easily detected, unlike the single massive target of the hull of the *Malta* in this survey (Bright et al. 2014:63-64). However, the majority of wooden shipwrecks off New Jersey were unarmed, and thus never had the ferromagnetic material aboard. In the same study of HMS *Fowey* performed by the Bureau of Ocean Energy Management and National Park Service in Biscayne National Park (Bright et al. 2014), several unarmed wooden vessels were surveyed with a towed magnetometer. Rigging hardware, iron fasteners, and small personal items presented small targets ranging from 5 nT to 20-40 nT in shallow water (less than ten feet deep), with magnetometer transects passing directly over the targets (Bright et al. 2014:64). Further complicating this situation is the fact that the majority of shipwrecks off New Jersey and elsewhere in shallow water were salvaged, sometimes very heavily, meaning that the maximum amount of ferromagnetic material thought to be aboard at the time of wrecking is no longer represented in the archaeological record due to anthropogenic causes, as described by O'Shea (2002:211-212) as a component of depositional theory under the formative theory component of the theory chapter in this thesis.

A second limitation is the nature of the inclusion of anthropogenic material into the New Jersey coastal environment, most notably in the form of outfall pipes and rock jetties and groins. Figure 26 from the *Rjukan* and Figure 28 from the *Sindia* clearly show the ends of outfall pipes as magnetic anomalies, which have the potential to obscure small ferromagnetic materials associated with shipwrecks. More significantly, the numerous rock jetties and groins along the New Jersey coast were constructed with iron and steel sheeting surrounded by rock. These objects present large magnetic anomalies, as seen in Figure 26 from the *Rjukan* flight area, with the potential to completely obscure shipwreck remains. As discussed in the introduction, the *Barnegat Inlet Shipwreck*, disturbed by the U.S. Army Corps of Engineers in 2014 during replacement of the north jetty of Barnegat Inlet, was directly under the 1930's-era jetty. It is completely possible that the magnetic signature of the jetty itself, as seen with the flight location of the *Rjukan*, could have totally obscured the magnetic signature of the deeper, buried shipwreck. This issue may not be as apparent when using a towed magnetometer array from a vessel, as the limitations on water depth would preclude the jetty and outfall pipes encountered in this survey from being in the vessel survey area.

Finally, natural and environmental factors can impact the effectiveness of UAV mounted surveys. UAVs cannot be flown over individuals not associated with their direct flight and operation, presenting significant challenges depending on the time of day and year. While this project occurred early in the spring, delays were still encountered due to pedestrians operating within the flight area. This could be mitigated with public closures of project areas, or by flying during off season hours. The wind is a significant factor, preventing flights over the *Sindia*, and is a significant consideration in the ability to fly over both land and water, especially when high winds bring large surf, requiring a higher flight elevation for platform safety. Additionally, many coastal areas are off limits from drone use to protect sensitive nesting shorebirds. Effective project timing can mitigate the challenge of nesting and migratory birds, but may lead to other negative impacts, such as pedestrian use and adverse weather conditions.

7.4 Future Applications

Additional datasets generated from continued survey applications will continue to show the effectiveness and define the operational detection parameters of the MAGPi ML-4. A focus on accessible, known, and well-documented wooden shipwrecks will provide the greatest calculations on capabilities of this system to find obscure and ephemeral wooden-hulled historic vessels at various depths below surface. If dimensions and tonnage are known of these sites, the potential to draw a correlation between tonnage and overall mass of wooden vessels and their ferromagnetic hull material exists. Future surveys should also establish the ability of the MAGPi ML-4 to identify historic shipwrecks concreted within coral formations, like those seen in Bermuda and other tropical areas, and determine the magnetic signature of widely scattered shipwrecks. In addition, projects such as the 2006 underwater survey of the James River by the National Park Service encountered zero-visibility, shoulder-deep water with a side-scan sonar speed limited to three knots. Further application of this aerial system to low energy river environments could increase the survey area, decrease the time needed, and result in safer conditions for team members (U.S. National Park Service 2018). Sites such as the periodically uncovered foundation remains of the Brigantine Life Saving Station, the collapsed remains of the Tucker’s Island, Egg Island, and Cohansey Lighthouses, and the remains of the shipbuilding industry of Dennis Township, all in New Jersey, provide additional magnetometer survey targets of the maritime cultural landscape within the littoral zone.

Drones and UAVs present one of the fastest growing platforms for archaeological research. The development of sensor arrays that include magnetometers, such as the MAGPi ML-4, with other remote sensing devices such as ground penetrating radar will allow for broad spectrum archaeological surveys in the challenging coastal environment. Continued public engineering projects to combat sea level rise ensure the need for continued identification of buried and submerged archaeological sites for project management purposes, and UAV operations provide one of the best abilities to detect and protect these vital components of our shared maritime cultural heritage.

Bibliography

Adams, Jonathan. (2003). Ships, Innovation and Social Change: Aspects of Carvel Shipbuilding in Northern Europe 1450-1850. Stockholm Studies in Archaeology No. 24. Stockholm Marine Archaeology Reports No. 3. University of Stockholm, Stockholm.

Allen, T. (2008). Sindia. The Wrecksite. https://www.wrecksite.eu/wreck.aspx?30724

Ashwell, J. (2020, March 28). Conservation Management Plan: The Lost Severn Trow William. https://www.academia.edu/42348021/Conservation_Management_Plan_The_Lost_Severn_Trow_William

Bass, George Fletcher and Frederick H. Van Doorninck. (1982). Yassı Ada. 1st ed. The Nautical Archaeology Series. Institute of Nautical Archaeology and Texas A&M University Press, College Station.

Berg, Daniel and Denise. (1993). *New Jersey Beach Diver*. Aqua Explorers, Inc. East Rockaway, New York.

Boshoff, J. (2018, January 1). The search for the slave ship Meermin : developing a methodology for finding inter tidal shipwrecks. https://www.academia.edu/72291637/The_search_for_the_slave_ship_Meermin_developing_a_methodology_for_finding_inter_tidal_shipwrecks?email_work_card=title

Bright, J., & Brown, D. (2013). *Analysis of Wooden Vessel Structure Remaining at BISC-0002*. 46th Annual Conference of the Society for Historical Archaeology.

Bright, John C., David Conlin, and Sage Wall. 2014. Marine Magnetic Survey Modeling: Custom Geospatial Processing Tools for Visualizing and Assessing Marine Magnetic Surveys for Archaeological Resources. US Dept. of the Interior, Bureau of Ocean Energy Management, Office of Renewable Energy Programs, Herndon, VA. OCS Study BOEM 2014-615. 240 pp.

CBS New York. (2014, November 4). Debris Found At Brick, N.J. Work Site Believed To Be From 1850 Shipwreck. CBS News. https://www.cbsnews.com/newyork/news/debris-found-at-brick-n-j-work-site-believed-to-be-from-1850-shipwreck/

Collins, A. R. (n.d.-a). *Armstrong-Frederick Gun Design of 1760*. Miscellaneous Technical Articles by Dr. A R Collins. http://arc.id.au/ArmstrongPattern.html

Collins, A. R. (n.d.). *British Cannonball Sizes*. Miscellaneous Technical Articles by Dr. A R Collins. http://arc.id.au/Cannonballs.html

Conlin, D., (1998), *Ship evolution, ship 'ecology' and the 'masked value hypothesis'*. IJNA, 27: 3–15.

Downey, Leland. (1983). *Broken Spars, New Jersey Coast Shipwrecks* 1640–1935. Privately published

Encyclopedia Britannica. (2019, August 8). littoral zone | marine ecology. Encyclopedia Britannica. https://www.britannica.com/science/littoral-zone

Flatman, J., & Staniforth, M. (2006). Historical Maritime Archaeology. In *The Cambridge Companion to Historical Archaeology* (pp. 168–188). Cambridge University Press. https://www.researchgate.net/profile/Mark-Staniforth/publication/32894250_Historical_maritime_archaeology/links/02bfe50ced80f38043000000/Historical-maritime-archaeology.pdf

Foley, J., Schultz, G., Helmke, M., Bochicchio, D., and Ennis, J., 2019, Enabling advanced miniaturized geophysical sensor systems through unmanned aerial vehicle Integration, American Geophysical Union Fall Meeting, San Francisco, NS11C-0649.

Ford, B., (2002), *The archaeology of maritime landscapes*. Springer.

Galiano, R. (2022). Malta. New Jersey Scuba Diving. https://njscuba.net/dive-sites/new-jersey-dive-sites/new-jersey-coast-chart/malta/

Gentile, G. (2000). *Shipwrecks of New Jersey: North*. Gary Gentile Productions.

Gibbins, David. (1990). Analytical Approaches in Maritime Archaeology: A Mediterranean Perspective. Antiquity 64:376-389.

Gibbins, D., & Adams, J. (2001). Shipwrecks and maritime archaeology. In *World Archaeology* (3rd ed., Vol. 32, pp. 279–291). Taylor & Francis, Ltd. https://www.jstor.org/stable/827923

Historic Naval Ships Association. (2022). ANCHOR-MAKING.-Vol. I. | Historic Naval Ships Association. https://www.hnsa.org/manuals-documents/age-of-sail/the-elements-and-practice-of-rigging-and-seamanship/anchor-making-vol-i/

Horlings, R. (2014, May 27). Of His Bones Are Coral Made: Submerged Cultural Resources, Site Formation Process and Multiple Scales of Interpretation in Coastal Ghana.

https://www.academia.edu/1029931/Of_His_Bones_Are_Coral_Made_Submerged_Cultural_Resources_Site_Formation_Process_and_Multiple_Scales_of_Interpretation_in_Coastal_Ghana

Hunter, J. W. (2004). The Phinney Site: The Remains of an American Armed Vessel Scuttled During the Penobscot Expedition of 1779. International Journal of Nautical Archaeology, 33(1), 67–78. https://doi.org/10.1111/j.1095-9270.2004.00006.x

James, Jr., S. R., & Gifford, E. (2015, May). CULTURAL RESOURCES INVESTIGATION DATA RECOVERY FOR BARNEGAT INLET NORTH JETTY UNANTICIPATED DISCOVERY BARNEGAT INLET, NEW JERSEY. US Army Corps of Engineers Philadelphia District & Marine Design Center Website. https://www.nap.usace.army.mil/Portals/39/docs/Civil/34164.m-Barnegat%20Shpwrk.pdf

Jaworski, J. (2019, December 20). *Unburied Treasure: Erosion from record high water levels reveals shipwrecks*. Glen Arbor Sun. https://glenarborsun.com/unburied-treasure/

Jordan, B. (2014, June 10). Archeological Overview and Remote Sensing Survey for Maritime Resources in Maryland State Waters from the Ocean City Inlet to the Delaware Line, Worcester County, Maryland. https://www.academia.edu/2172013/Archeological_Overview_and_Remote_Sensing_Survey_for_Maritime_Resources_in_Maryland_State_Waters_from_the_Ocean_City_Inlet_to_the_Delaware_Line_Worcester_County_Maryland

Keith, A., & Evans, A., (2002). Modeling maritime culture: Galveston, Texas, in the historic period. In B. Ford (Ed), *The archaeology of maritime landscapes* (pp.179-194). Springer.

Lettens, J. (2008, February 2). SV Malta. The Wrecksite. https://www.wrecksite.eu/wreck.aspx?20540

McConnell, D. (1988). British smooth-bore artillery : a technological study to support identification, acquisition, restoration, reproduction, and interpretation of artillery at national historic parks in Canada / David McConnell.: R64-178/1988E-PDF - Government of Canada Publications - Canada.ca. Government of Canada. Retrieved September 16, 2022, from https://publications.gc.ca/site/eng/9.889116/publication.html

Meide, C. (2013). *The Development of Maritime Archaeology as a Discipline and the Evolving Use of Theory by Maritime Archaeologists*. https://www.academia.edu/4376520/The_Development_of_Maritime_Archae ology_as_a_Discipline_and_the_Evolving_Use_of_Theory_by_Maritime_Archaeologists

Matrice 600 Pro - Product Information - DJI. (2022). DJI Official. https://www.dji.com/matrice600-pro/info

Meide, C. (2016). Bang Bang! Cannons, Carronades, and the Gun Carriage from the Storm Wreck. ACUA Underwater Archaeology Proceedings 2016, 142–152.

Muckelroy, Keith. (1978). Maritime Archaeology. New Studies in Archaeology Series. Cambridge University Press, Cambridge

Nagiewicz, S. (2016). *Hidden History of Maritime New Jersey*. The History Press.

National Park Service (n.d.). *Magnetic Moment Calculator*. Microsoft Excel Spreadsheet.

New Jersey Maritime Museum. (2021). *Shipwreck Database.* https://docs.google.com/spreadsheets/d/1xJLGc5VjYmqh0xA14oSGs9_DoPKSdeh78AHa7CyMe4E/edit#gid=540543533

Noble, Dennis L. (1994). That Others Might Live: The U.S. Life-Saving Service, 1878–1915. Naval Institute Press.

North Carolina Department of Natural and Cultural Resources. (2021). Arms and Armament. Queen Anne's Revenge Conservation Lab. https://www.qaronline.org/conservation/artifacts

O'Connor, E. (2012, November 18). Sandy Exposes 90-Year-Old Shipwreck on Fire Island. TIME.Com. https://newsfeed.time.com/2012/11/18/sandy-exposes-90-year-old-shipwreck-on-fire-island/

O'Shea, J., 2002, The archaeology of scattered wreck□sites: formation processes and shallow water archaeology in western Lake Huron, *International Journal of Nautical Archaeology*, 31:2, 211-227, DOI: 10.1111/j.1095-9270.2002.tb01415.x

Price, F., Dilk, S., & Brooks Jr, B. (2014). The Seal Cove Shipwreck Project: Investigating an Historical Wooden Vessel on Mount Desert Island, Maine. Northeast Historical Archaeology, 43, 130–151. https://orb.binghamton.edu/cgi/viewcontent.cgi?article=1420&context=neha

Richards, N. (2016, October 27). Shipwrecks of St. John: ECU Investigations of Submerged Cultural Resources in the U.S. Virgin Islands National Park, 2002. https://www.academia.edu/29469000/Shipwrecks_of_St_John_ECU_Investig ations_of_Submerged_Cultural_Resources_in_the_U_S_Virgin_Islands_National_Park_2002

Russell, M. (2002). Beached Shipwrecks from Channel Islands National Park, California. Journal of Field Archaeology, 29(3/4), 369–384. https://doi.org/10.2307/3250898

Saraceni, J. E. (2020, November 18). Erosion Exposes Shipwreck on Florida Beach - Archaeology Magazine. Archaeology. https://www.archaeology.org/news/9218-201118-florida-beach-shipwreck

Schultz, G., Helmke, M., Masters, A., & Keranen, J. (2021, September 22). *Unmanned Aerial System Magnetic Sensing for UXO Site Assessments*. FastTIMES Online. https://fasttimesonline.co/unmanned-aerial-system-magnetic-sensing-for-uxo-site-assessments/

Sindia 037, Ocean City, NJ, postmarked Aug. 4, 1917. (2015, November 11). Historical Society of Riverton, NJ. Retrieved September 16, 2022, from https://rivertonhistory.com/images/ocean-city-nj-images/sindia-037-ocean-city-nj-postmarked-aug-4-1917/

Southeastern Archaeological Research, Inc. (2010, April). UNDERWATER ARCHAEOLOGICAL INVESTIGATION OF THE ROOSEVELT INLET SHIPWRECK (7S-D-91A) VOLUME 1: FINAL REPORT. https://history.delaware.gov/wp-content/uploads/sites/179/2019/02/volume1.pdf

Thompson, B. (2005, November). The Martinak Boat (CAR-254, 18CA54) Caroline County, Maryland. Maryland Department of Planning Maryland Historical Trust, Office of Archeology Maryland State Historic Preservation Office. https://mht.maryland.gov/documents/pdf/archeology/currentresearch/martinak.pdf

U.S. National Park Service. *Underwater Survey at Colonial NHP*. (2018, August 2). National Park Service. https://www.nps.gov/articles/underwater-survey-at-colonial.htm

Vanhorn, K. M. (2004, December). EIGHTEENTH-CENTURY COLONIAL AMERICAN MERCHANT SHIP CONSTRUCTION. Texas A&M University. https://nautarch.tamu.edu/Theses/pdf-files/VanHorn-MA2004.pdf

Walker, B. C. (2001). Lab 5: Superposition of Magnetic Fields. University of Delaware, Department of Physics and Astronomy. https://www.physics.udel.edu/~nowak/phys208/Labs/SuperpositionFields.pdf

Westerdahl, Christer.

(1986). Die maritime Kulturlandschaft. Schiffe, Schiffahrtswege, Häfen. Überlegungen zu einem Forschungsansatz. Deutsches Schiffahrtsarchiv 9:7-58.

(1992). The Maritime Cultural Landscape. International Journal of Nautical Archaeology 21(1):5-14.

White, R. (2019, November 29). *Storm surge on Lake Michigan uncovers shipwreck off Muskegon coast*. WZZM13. https://www.wzzm13.com/article/news/local/lakeshore/muskegon-shipwreck-uncovered/69-22f32c5b-7a24-43a5-aaa1-b301b81cc7d1?fbclid=IwAR3pLSV2QjKhTKff3YEa3-QY6Q659ym19SQyHDV2tx1XVtOZVpsDU-Y3ozY

Zwick, D. (2021, July 12). A late 17th-century "Double Dutch" construction in the North Frisian Wadden Sea: the case of the Hörnum Odde wreck on the island of Sylt, Germany. https://www.academia.edu/49788749/A_late_17th_century_Double_Dutch_construction_in_the_North_Frisian_Wadden_Sea_the_case_of_the_H%C3%B6rnum_Odde_wreck_on_the_island_of_Sylt_Germany